LOCALISED CORROSION

OF

AUSTENITIC STAINLESS STEELS

LOCALISED CORROSION

OF

AUSTENITIC STAINLESS STEELS

by

Gyanendra Kumar Jha, B.Tech. (Hons)

A Thesis

Submitted to the School of Graduate Studies

in Partial Fulfilment of the Requirements

for the Degree

Master of Engineering

McMaster University

August 1971

MASTER OF ENGINEERING (1971) McMASTER UNIVERSITY

(Metallurgical Engineering) Hamilton, Ontario.

TITLE: Localised Corrosion of Austenitic Stainless Steels

AUTHOR: Gyanendra Kumar Jha, B.Tech. (Hons) (I. I. T., Kharagpur)

SUPERVISOR: Professor M. B. Ives

NUMBER OF PAGES: v, 85

SCOPE AND CONTENTS:

The localised corrosion behaviour of various grades of Austenitic Stainless Steels has been demonstrated by optical and electron microscopy. The effect of sensitisation upon subsequent corrosive attack has been investigated. A theoretical model based upon thermodynamic and kinetic considerations has been proposed to account for the observed experimental results.

ACKNOWLEDGEMENTS

The author is indebted to his supervisor, Dr. M. B. Ives, for continued guidance during the various stages of this research. He wishes to express his appreciation to Dr. J. S. Kirkaldy and Dr. G. R. Purdy for helpful discussions during the latter stages of this work.

He acknowledges the assistance and co-operation of his various colleagues. In particular, thanks are due to Mr. M Zamin for his constant help. Thanks are extended to all the technicians of the department, particularly to Mr. Tibor Tandi for his invaluable assistance in Electron Microscopy.

He acknowledges the receipt of financial assistance from McMaster University in the form of scholarship-cum-assistantship.

TABLE OF CONTENTS

INTRODUCTION

Austenitic stainless steels, as a class, are generally regarded as materials with remarkable corrosion resistance properties - only the noble metals compare with them. They rely mainly on their "surface passivity" for resisting corrosive attack.

But even these steels can loose their passive behaviour, either locally or throughout the surface exposed, under certain specific conditions. An attempt will be made to study these localised corrosion phenomena of Austenitic stainless steels.

Generally, any metallic material is subjected to one or more of the following eight modes of corrosion [1]; (1) Uniform or General attack, (2) Galvanic or two metal attack, (3) Crevice Corrosion, (4) Pitting Corrosion, (5) Intergranular Corrosion, (6) Selective Leaching or Parting, (7) Erosion - Corrosion, (8) stress Corrosion.

Crevice Corrosion, Pitting Corrosion and Intergranular Corrosion are three aspects of localised Corrosion, which gain added importance when consideration of stainless steels is made. Pitting Corrosion, has been regarded by many as a specific case of Crevice Corrosion.

The mechanism of Pitting and Intergranular corrosion of Austenitic stainless steels and their dependence upon various factors such as chemical composition, heat treatment, environmental factors, such as the corrosive media will be discussed. The basic methods of determining their initiation and propogation in these steels will be reviewed critically.

An attempt to correlate the various factors controlling these two forms of localised corrosion in Austenitic stainless steel will be made.

CHAPTER I

PART A: PITTING CORROSION OF AUSTENITIC STAINLESS STEEL

(a) THEORY OF STAINLESS STEEL PITTING

The surface of stainless steels can exist in three different electro-chemical states; active, passive and transpassive. (Figure 1). In the active and transpassive states uniform corrosion attack takes place. In the passive state, corrosion rate is greatly inhibited and is nearly zero.

Under certain conditions the passive behaviour of either the whole surface or particular spots can be lost, so that very formidable localised corrosion phenomena may occur. An example of such localised corrosion is pitting caused under certain conditions by chloride ions. When testing for susceptibility to pitting corrosion, the most important and critical consideration is not the corrosion rate, but rather the conditions under which pitting corrosion may or may not occur. Under pitting corrosion conditions the material may be penetrated and rendered useless, even if there is a low corrosion rate.

Pitting may be divided into two distinct steps:

(a) Pit initiation or surface breakdown and

(b) Pit growth in depth and volume.

Although the factors determining pit initiation are largely unknown, and at times the reported works seem to be contradictory, pit growth has been described in quite a detailed manner in the available literature.

The intensity of localised attack which leads to the growth of deep pits result from several factors. The pit is the anode, and the unaffected area surrounding the point of penetration is the cathode of a cell whose electrolyte is the corrosive solution. (Figure 2). On metals covered by protective passive films, the surface area available for cathodic reactions is very large compared with that for anodic reactions, which takes place at the point or points of breakdown in the film. As a result, the current per unit area of cathode surface remains low, and large areas may be exposed to cathodic reaction accelerators in the solution. e.g. oxidising agents which depolarise this reaction and thereby stimulate the anodic reaction. Anodic dissolution may also be stimulated by reduction of ferric to ferrous ions at cathodic areas.[2]

The anodic current density is high, and enough material is soon removed to form a depression in the surface, unless corrosion products stifle the reaction. In some cases, oxygen combines with metal ions produced by corrosion to form protective oxide films. (This aspect will be considered in more detail when dealing with the phenomena of passivity). However, if there is insufficient oxygen available, or if the oxides formed are not protective the pit grows. A cavity is soon formed in which oxygen is not easily replenished, and is, therefore, soon exhausted. Also, the corrosion current causes any chloride ions present to migrate to the anodes.[3] These ions tend to destroy the protective qualities of any film, which may still be present and will acidify the solution in the pit. The combination of large cathodic and small anodic areas, oxygen exhaustion, chloride ion accumulation, and

acid conditions produces an intensely localised form of attack.

Oxygen plays a dual role by its ability (a) to stifle the anodic reaction by film formation and (b) to accelerate the cathodic process by removal of hydrogen and by regenerating ferrous to ferric ions. Both these effects may be operative at the same time or independently. The overall result on the corrosion rate i.e. the kinetics of pitting process, depends on whether anodic retardation or cathodic stimulation is dominant.[4] For example, in a study of pitting corrosion on straight chromium (17% Cr) stainless steel in sea water [5] the amount of corrosion in the pit was directly proportional to the uncorroded cathodic area surrounding the pit. As long as the amount of oxygen available per unit area of cathode exposed to flowing sea water was constant, the extent of stimulation depended only on the size of the cathodic area. But, in another investigation,[6] pitting of Type 304 stainless steel in sodium chloride solutions exposed to atmosphere was almost completely suppressed when oxygen was removed. Oxygen was acting as a cathodic stimulant. However, when the oxygen pressure was increased to 60 atmosphere, pitting was also retarded, because at this pressure the film forming properties of oxygen became dominant.

(b) ELECTRO-CHEMICAL ASPECTS OF PITTING CORROSION OF STAINLESS STEEL

Rosenfeld and Danilov[7] suggest that a pit should not be considered to be relatively deep, uncovered region of preferential attack (Figure 3a).

Pits in stainless steel are relatively closed corrosion zones. A chloride ion penetrates under the surface metal layer and then the corrosion process developes in a closed zone as shown in Figure 3b. Microscopic examination reveals a small sized hole which is the result of the destruction of the passive film. Under such circumstances, access of the passivator required to maintain the passive state in the pit is hampered and opposed by the diffusion process. As far as the effect of the electric field strength is concerned[7], a rapid differentiation of the surface into local anodes and cathodes prevent the passivator (Fe^{+++}) from penetrating into the pit and thereby speeds up the transfer of the activator - $C\ell$ - to the pit. Consequently, the pit is a peculiar crevice, where, as a result of the insufficient access of the passivator, favourable conditions are created contributing to the high speed development of the anodic process.

Experimental evidence based on this mechanism has been furnished by Danilov[7] wherein it is suggested that pitting corrosion is a specific mode of crevice corrosion where the electrochemical behaviour of the metal is caused only by the difference in the access of the corrosive medium and in the removal of the corrosion products. Pitting corrosion will stop if the pit and the rest of the surface were equally accessible to the electrolyte. Experiment has confirmed this hypothesis.

Destroying the shielding layer over the pit with resultant free access of the solution from the bulk appear to lead to the direct passivation of the pit metal and to the equalisation of the potential. This leads to the termination of the pit.

(c) LOCATION OF THE ORIGIN OF PITS

There are contradictory arguments available regarding the favoured sites for pit nucleation in Austenitic stainless steels.

Rosenfeld and co-workers [7] are not in favour of accepting the concept of a certain limited number of sites sensitive to pitting corrosion; these centres corresponding to points of structural defects or compositional inhomogenity. Their investigations show that if the first pits are opened up and therefore made easily accessible to the passivator then the number of pits become very high. The concept of limited number of pits appearing on the centres sensitive to pitting corrosion seems doubtful, for, if such would have been the case, the above workers argue, then if those pits were opened up and made accessible to the passivator, they would passivate and new ones would have originated on these very points, which is in contradiction to their experimental findings. They argue that there are a great number of such centres, but owing to the protective action of the first pits, new pits are not formed. This view point is indirectly supported by the work of Evans [9] and that of Mears and Brown [10]. Evans suggests that the existence of a vigorous pit at one point makes conditions unfavourable to the development of pits at points around. If two pits are hypothetically considered to exist close to one another, both will compete for the

corrosion current available and therefore will have a smaller chance of developing the autocatalytic mechanism (to be discussed in the subsequent section) needed for continued corrosion than a single isolated pit. However, there is a more general reason. The high anodic density at a vigorous pit shifts the potential in such a direction as will reduce the available E. M. F. and the whole potential distribution in the solution will be altered in such a way as to make conditions less favourable to attack at points around. In other words, the probability of the depth of a pit which is isolated from others being more is higher than that of a pit which grows in a cluster which has to compete for survival.

But, Schwenk [11] is of the opinion that pits formed are greatly dependent upon the bounding planes. His analysis of these pits lead to the conclusion that the pits bounding the planes belonging to (111) the planes that are most densely packed for austenite. The crystallographic planes with the lowest dissolution rate form the bounding planes - which happen to be (111) for Austenitic stainless steels. This view point has been refuted by Ives [12] who has stated that very few examples of etch pits exhibiting crystallographic low-index faces have been seen.

The present work which was undertaken shows that the origin of pit nuclei is greatly dependent upon the thermal history of the specimen. Thus an Austenitic stainless steel which is solution quenched from 1300°C and subjected to corrosive attack in ferric chloride solution shows pit nucleation at random sites throughout the area of the specimen exposed. But, on the other hand, if the specimen is sensitised at 650°C after the above solution quenching then the density of pitting is greater along the

grain boundaries than in the grain interior. The reason for this has been provided in the discussion of the experimental work.

(d) AUTO CATALYTIC NATURE OF PITTING CORROSION

Pitting corrosion is essentially an anodic reaction which is autocatalytic in nature.[1] That is, the corrosion processes within a pit produce conditions which are both stimulating and necessary for the continuing activity of the pit. This is illustrated in Figure IV. The metal M is being pitted by an aerated sodium chloride solution. Rapid dissolution takes place within the pit, while oxygen reduction takes place on adjacent surfaces. This process is self-stimulating and self-propogating. The rapid dissolution of metal within the pit tends to produced an excess of positive charge in this area, resulting in the migration of chloride ion to maintain electro-neutrality. Thus in the pit there is a high concentration of MCl, and as a result of hydrolysis a high concentration of hydrogen ions. Both hydrogen and chloride ions stimulate the dissolution of most metal and alloys and the entire process accelerates with time. The solubility of oxygen is virtually zero in concentrated chloride solutions, so as oxygen reduction occurs within a pit. The cathodic oxygen reduction on the adjacent surfaces to the pit tends to suppress corrosion. THUS THE PIT CATHODICALLY PROTECTS THE REST OF THE METAL SURFACE.

According to Evans [9] the initiation and the subsequent auto-catalytic propogation of the pit could be based upon the following theoretical model. Consider a piece of metal or alloy, say austenitic stainless steel - immersed in aerated chloride solution. If for any

reason the rate of dissolution is momentarily high - say due to breakdown of the surface passivity by a scratch, emerging dislocations or random variation in solution composition - then chloride ions will migrate to that point where the breakdown has occurred. During the initiation or early growth stages of a pit, conditions are unstable. The locally high concentration of chloride or hydrogen ions may be swept away by local convection currents in the solution. The instability of the pit initiation has been demonstrated by Schwenk [11] and Evans.[9]

(e) KINETICS OF PITTING CORROSION

A theoretical model, under potentiostatic conditions has been proposed by Engell, Stolica and Schwenk.[11,13] Although such a model has some serious limitation, yet it is worthwhile being reviewed:

Postulates

(i) Current increases as the square of time in the case of undisturbed corrosion:

$i = c\ t^2$ - (1) where c is constant

(ii) For pit growth

$i = a\ r^2\ j\ Z$ - (2)

where a = constant, r = radius of pit, j = current density in the bottom of the pit, Z = no. of pits.

(iii) Integrating Equation (2)

$$\int_0^t i\ dt = {}_b\ r^3\ Z \quad - (3)$$

where b is constant

Based on Equations (1), (2) and (3) the value of the constant c is found as:

$$c = \frac{i}{t^2} = \frac{a\, r^2\, j\, Z}{t^2} = \frac{a^3}{9\, b^2}\, j^3\, Z \quad - (4)$$

(iv) This shows that the constant c is an explicit function of potential, which would become readily apparent by considering a constant current and then combining equations (1) and (4).

$$\frac{-2\, d \ln t}{dE} = \frac{3\, d \ln j}{dE} + \frac{d \ln Z}{dE} \qquad (5)$$

(v) The above workers have shown that the pitting density changes at a very insignificant rate with the change in Potential till a value of 700 mv. Thus the second term in the above expression $\frac{d \ln Z}{dE}$ may be neglected.

$$\frac{dE}{d \ln j} \leqslant -\frac{3}{2} \frac{dE}{d \ln t} \qquad (6)$$

Thus, the rate of change of potential with current density will never be more than one and a half times the rate of change of potential with the log. of time. This finding has been experimentally confirmed by Engell, Stolica and Schwenk[11,13].

From equation (5) it follows that the pitting density and Current density in the pit bottom are independent of potential. This result agrees with the experimental investigations of Engell and Stolica (13), for pure iron at potentials above 850 mv_H.

Limitations of the Above Model:

(i) Potential-time curves, in most cases, are not reliably representative. The induction period strongly increases with current density.

(ii) Within the Pitting Potential range, some irregular variations occur which are oscillatory in nature. This has been critically examined by Rosenfeld[7] and has been attributed to the repassivating tendencies of the system.

(iii) Counting of the pits for purposes of reproducible analysis may not be practically possible. Despite the above limitations, the above model gives a fairly satisfactory picture regarding the growth of pits and its dependence upon various electrochemical and physical parameters.

(f) FACTORS AFFECTING PITTING CORROSION OF AUSTENITIC STAINLESS STEELS

The factors affecting pitting of austenitic stainless steels may be grouped under the following representative headings:

I Metallurgical Factors

The most significant factors are:

(i) The carbon content and presence of alloying elements and the associated case of differential composition or concentration;

(ii) Heat Treatment;

(iii) Grain size, orientation of grains;

(iv) Presence of twin boundaries particularly the incoherent ones.

II Chemical and Environmental Factors

(i) Effect of activators such as chloride ions in the corrosive medium and solution concentration.

(ii) Effect of Inhibitors

(iii) pH of the medium

(iv) Temperature

(v) Composition changes in the medium during reaction.

(vi) Conditions of agitation and stagnation.

(vii) Surface finish

III Electro-chemical Factors

(i) The passivating ability of the alloy.

(ii) Potential across the "double-layer".

I. Metallurgical Factors

(i) Effect of Alloying Elements

	Elements	Effect on Pitting Resistance
Adverse Effect	Carbon	Decreases resistance to pitting particularly in the sensitised condition.[1,14]
	Sulfur and Selenium	Decreases[14,15]
	Silicon	Decreases[14,16] - but improves when present with Molybdenum (to be further explained when dealing with Passivity.)
Beneficial Effect	Chromium	Increases
	Nickel	Increases
	Molybdenum	Increases[1,16]
	Nitrogen	Increases

The works of Streicher[17] and of Tomashov[14] suggests that pitting mainly occurs at the grain boundaries. This strongly indicates a positive correlation between pitting and intergranular corrosion, an aspect which will be considered in some detail at a later point. Tomashov and co-workers[14] suggest that those elements capable of increasing stability of their "passive state" (?) increase the resistance of the steel to pitting corrosion. The elements belonging to this class are nickel, chromium, Molybdenum and nitrogen. The positive effect shown by these elements is, as suggested by Tomashov[14] and Rhodin,[16] due to a more

stable homogeneous structure. Tomashov is of the opinion that pitting may be due to the precipitation of secondary phases resulting in the heterogeneity of metal composition. The more homogeneous the structure, more will be the resistance to pitting corrosion. In the presence of ferritic inclusions austenitic stainless steels become increasingly susceptible to localised corrosion.[14]

To date, there is still no clear cut answer to the question whether the primary effect of the alloying elements is to reduce the probability of development of pits in the initial corrosion sites, or whether the effect is purely that of retardation of the rates of development of these sites. An attempt will be made to critically discuss this problem based upon the present work.

I. (ii) Effect of Thermal treatments on Pitting Corrosion

The works of Fontana and Greene[1,18] and that of Tomashov and co-workers[14] suggest:

(a) Heating an austenitic stainless steel at 650°C (sensitising range) for an extended period of time, say 2 hours, strongly enhances susceptibility to Pitting Corrosion. Experiments were carried on 1.8 Cr - 14 Nr steel with and without Mo, V and Si.[14]

(b) The above steels with as high as 5% Mo, Si, and V, which were otherwise stable in the solution-quenched state in Ferric chloride solution, corroded strongly, with pitting confined to grain boundaries.

(c) It is suggested that the above increased susceptibility to pitting corrosion by heating in the"sensitising zone" is due to the

structural heterogeneity resulting as a consequence of the above treatment. The heterogeneity increases the probability of pit initiation due to the availability of an increased number of anodic sites.

I (iii) Grain Size

Smaller the grain size of the austenite matrix, greater will be the ratio of grain boundary area to the total area, and thus greater will be the anodic dissolution sites which would increase the number and rate of pitting.

I (iv) Twin-Boundaries

It has been observed in course of the present work that pits preferentially nucleate at incoherent twin-boundaries, particularly in the sensitised condition. It is suggested, that the incoherency strains associated with the above is largely responsible for lowering the activation energy needed for pit-formation at these sites.

II Chemical and Environmental Factors

(i) Effect of Activators such as Chloride Ions in the Corrosive Medium

An essential condition affecting pitting in the presence in the solution of one of the specifically acting anions, particularly $C\ell^-$, Br^- or I^-. The presence of $C\ell^-$ ions facilitates pit formation to the greatest extent[1,17,18]. The possible role which chloride ions play in the anodic behaviour of alloys such as austenitic stainless steel can be explained on the basis of the following model of Taube[21] and Vijh[20].

According to Taube, co-ordination complexes such as chloro-complexes are formed by ions of various metals of interest. Complexes in which d-orbitals are hybridised with S and p orbitals of the next higher principal quantum number are called INNER ORBITAL COMPLEXES. Conversely, complexes which do not involve hybridised d-orbitals are referred to as OUTER ORBITAL COMPLEXES. Energetically, inner orbital complexes are a configuration of greater energy of co-ordination, than are the outer orbital complexes because inner orbitals represent lower energy levels than the outer orbital. It has been shown by Taube that the chloro-complexes of metals like Fe and Al are of the outer orbital type whereas those of metals like Ti, Zr, Mo and W are of the inner orbital type.

Case A. Corrosion of a Metal or Alloy of the OUTER ORBITAL TYPE (Fe).

$$M + n\,C\ell^- \longrightarrow M(C\ell)_n + ne \qquad \text{(i)}$$

$$M(C\ell)_n \longrightarrow M^{n+} + nC\ell^- \qquad \text{(ii)}$$

$$M^{n+} + mC\ell^- \rightleftharpoons (McC\ell_m)^{(m-n)e} \qquad \text{(iii)}$$

This being an outer orbital complex is not stable and thus it dissociates back to the reacting ions:

$$(Mn\ C\ell_m)^{(m-n)e} = M^{n+} + mC\ell^- \qquad \text{(iv)}$$

This dissociation process would make chlorine available again and set a cycle of reactions (i) to (iv). This indirectly explains the autocatalytic nature of pitting.

Case B. Corrosion of a Metal of the INNER ORBITALS TYPE (e.g. Molybdenum)

For metals like Mo, Zr, Ti, etc. the complex $(M_nCl_m)^{(m-n)e}$ is very stable, being of the outer orbital type, thus the regenerative reaction (iv) is prevented. The complex thus, effectively scavanges the Cl^-, and thus prohibits these ions form further participation in the anodic charge transfer reaction.

Solution Concentration: Pitting will occur only if the "agressive ions" mentioned above are present beyond a certain critical concentration. For example, Engell and Stolica[13] observed that the formation of pits on a passive iron surface can occur only if chloride ion concentration is greater than 3×10^{-4} mg/litre. The critical ion concentration will depend upon:

(a) Nature of metal and alloy

(b) Its thermal treatment

(c) State of its surface

Oxidising Agents: Pitting corrosion in solution containing "agressive ions" such as chloride ions occur only in the presence of oxidizing agents such as Fe^{+++}, Hg^{++}, Cu^{++}, H_2O_2, dissolved oxygen, etc.[22] Kolotyrkin states that the oxidising agents have a depolarising action which when reduced on the metal surface shifts its potential in the positive direction. The stimulating action of the pitting corrosion depends upon the nature and concentration of the oxidising agents, nature and concentration of the agressive ion and the nature and state of the corroding metal.

II (ii) Effect of Inhibitors or "Unaggressive" ions

Certain inhibitors such as nitrates in chloride ions greatly retard the rate of pitting corrosion. Work of Uhlig[2] shows that the introduction of nitrates in comparatively small concentrations can prevent completely the formation of pits. He demonstrated that no pits are formed on grade 304 stainless steel immersed in 10% $FeCl_3$ containing 3% $NaNo_3$ where it dissolves at one millionth of its rate in pure $FeCl_3$. Similar results were obtained by Fontana and Green[18], who showed that an artificialpit made by them could not be activated in 0.1 N $FeCl_3$ if it contained $NaNO_3$ in the concentration of 0.05 M. Streicher [17] has shown that the minimum concentration of nitrates necessary for inhibiting pitting stainless steel depends greatly on the type of steel as well as the method by which the surface is treated.

II (iii) pH of the Medium

Alkalis have an inhibiting effect upon pitting corrosion. Susceptibility to pitting is reduced by increasing the pH value.[17] However, some contradictions are present in the literature regarding the effect of pH. Odd Steensland[23] took potentiostatic tests to determine the true position of the pitting potential in relation to the pH value of a 5% $NaCl$ solution. This shows that the pitting potential increases with pH value. On the other hand, Hospadarnu found that pitting potential of AISI type 301steels was practically unrelated to pH value up to 8, in the case of $NaCl$.[24] But in $CaCl_2$ solution, the pH value had a marked influence on pitting potential. What practically amounts to the reduction in pitting with the increase in the solution's pH value is

attributed to a shift in the cathodic branch of the current density potential curve to smaller potentials with simultaneous rise in pH.

II (iv) Effect of Temperature

Based upon the work of Uhlig[25] and Rosenfeld[26] the following conclusions are drawn. Stainless steels with and without Mo showed an increase in the number of pits with rise in temperature. The increase in number of pits was explained in terms of increased reactivity of chlorine ions facilitating their chemical adsorption on the surface of steel.

II (vii) Surface Finish

Besides the above factors, surface finish of the steel may affect pitting. Apart from localised breakdown of the protective film, the pitting may begin at weak points of the metal surface. Pit nuclei formation is often increased by mechanical working of the metal, by local cold work in particular. Surfaces having rough finish are more susceptible to pitting than those which are highly polished.

According to the work of Steensland[23], the following result was obtained for AlSl 304 carried out in 5% NaCℓ solution into which oxygen was blown to determine the true pitting potential in relation to various surface finish:

Mechanically Polished - Maximum susceptibility

Pickled and Passivated - Intermediate susceptibility

Electrolytically Polished - Least susceptibility.

III Electro-Chemical Factors

(i) The Role of Passive Films

The presence of passive films upon the surface of certain metals and alloys, including austenitic stainless steels, exert a critical effect upon the localised corrosion behaviour of these alloys. Though a number of theories are available in literature regarding the concept of passivity, yet none of them clearly explain the exact role and nature of passivating films in resisting corrosion.

Passivity is a property of a metal or an alloy commonly defined in two ways. One of them is based upon the change in electro-chemical behaviour of the metal, and the other on its corrosion behaviour. The definitions may be stated as follows:[25]

Definition 1 A metal active in the E.M.F. series, or an alloy composed of such metals, is considered passive when its electro-chemical behaviour becomes that of an appreciably less active or noble metal.

Definition 2 A metal or an alloy is passive if it substantially resists corrosion in an environment, where thermodynamically, there is a large free energy decrease associated with its passage from the metallic state to appropriate corrosion products.

Passivity is not an absolute property like specific heat, or heat of fusion. An alloy may possess variable degrees of passivity. The degree of passivity is measure by (1) Galvanic Potential: Only for metals and alloys passive by definition. (2) Corrosion rate.

1. A more noble potential of a metal can result from either passi-

vation or from anodic polarisation through local action currents of a hetrogeneous surface containing more noble potential. Thus, adequate interpretation of potential measurements as evidence of passivity must take into account the latter possibility.

(2) Reaction or Corrosion Rate: In general, oxidising conditions favour passivity while reducing conditions destroy it or cause activity. For example, anodic polarisation passivates iron, whereas cathodic polarisation, activates or destroys passivity in iron. Reducing solutions in general act in the same manner as cathodic polarisation. A metal or an alloy in contact with a more noble metal (corresponding to anodic polarisation) is more easily passivated, but in contact with a less noble metal, cathodic polarisation occurs and passivity is more difficult or impossible to attain.

Theories of Passivity

Generalised Film Theory

Many theories of passivity have been proposed. The earliest seems to be that of Faraday[46], who apparently considered the passivity of iron in nitric acid "to be attributable to the formation of an oxide film". This oxide film theory of Faraday has been generalised, and the so-called film theory, is the one most widely used at present. Evans[9] has stated it as follows: "Most cases of passivity... appear to be attributable, directly or indirectly to a protective film, though not always an oxide film". Similar views have been expressed by Glasstone[47] and Mears.[48]

This generalised film theory embraces the special cases where a film of oxygen rather than the oxide causes passivity. However, Tammann[49] later suggested that a film of adsorbed oxygen, rather than the oxide is responsible for the passivity of Iron, Nickel, Cobalt, Chromium, and austenitic stainless steels.

The Electron - Configuration Theory

A theory has been proposed by Uhlig[45] which attempts to correlate many of the above mentioned theories with some aspects of the generalised film theory.

There exists a relation between electron configuration and passivity. Metals passive according to definition I are largely those in the transition groups of the Periodic table. The atoms of these metals according to the Electron Theory of Metals, e.g. Chromium,

Nickel, Cobalt, iron, Molybdenum and Tungsten, are characterised by incomplete inner d-shells. The electron configuration theory assumes that these unfilled energy states tend to fill with electrons in the same manner as the tendency of having closed atomic shells in chemical compounds. The state of passivity is ascribed to the condition of unfilled d-bands, and the active state to the situation that, in effect, fills the d-bands with electrons. Thus, adsorbed oxygen or adsorbed oxidising substances accompany maximum passivity because they are electron absorbers with no tendency to supply electrons to atoms of the metal surface. On the other hand, interstitial hydrogen (by pickling or cathodic polarisation) or certain classes of alloying elements in adequate concentration supply electrons and thereby favour the active over the passive state.

In stainless steels, the constituent chromium is naturally passive and is considered to impart this property to iron by electron sharing resulting from the strong tendency of chromium to absorb electrons. This assumption is supported by the fact that active iron as an anode in an electrolyte , (e.g. sodium sulphate) corrodes as Fe^{++} but from passive stainless steel it corrodes as Fe^{+++}, i.e. with one electron less. Similarly, chromium with five vacancies in the 3d shell of the atom has a corresponding number of vacancies in the 3d band of the metal. With a stronger tendency than iron to absorb electrons, it can share at least 5 electrons or can passivate 5 iron atoms. This proportion corresponds to 16.7 atomic per cent or 15.7 weight per cent chromium which is in satisfactory agreement with the observed critical minimum amount of chromium, about 12% necessary to produce the so called stainless Cr-Fe alloys.

The mechanism for the ennobled potential and reduced reactivity of passive metals and alloys is considered to reside largely in the surface - metal atoms. It is the electron configuration of surface metal atoms that determines whether an approaching substance, say an anion, will react or not. If it reacts, a protective layer of reaction product may form on the surface, accounting for passivity by definition 2, but not for passivity with which the electron configuration theory is concerned - definition 1. If the substance does not react, it will ADSORB on the metal surface because of existing affinities. In so doing it satisfies secondary valence forces of the metal surface and displays in itself considerably less chemical affinity for substances impinging on the adsorbed layer. The metal surface is therefore less reactive and by this mechanism is considered passive.

The condition that determines whether an ion capable of reaction with the metallic surface will react or will prefer to be adsorbed appears to be related to the ratio of work function of the metal (a measure of the heat of evaporation of the electrons from a metal) and the heat of sublimation of the metal. When oxygen approaches a metal surface, two distinct possibilities exist: - (a) It will either extract an electron from the metal surface and become adsorbed or (b) a metal atom will be dislodged from the most vulnerable point in the lattice to form an oxide. The preferred process, from the thermodynamic stand point is one which is associated with a greater decrease of free energy.

Thus, for passivity $\dfrac{\text{work function}}{\text{Heat of sublimation}} < 1$

for reaction $\dfrac{\text{work function}}{\text{Heat of sublimation}} > 1$

Alloying, which affects both the work function and the sublimation energy can induce eitherpassivity or activity depending upon the ratio of these quantities at any alloy composition.

Breakdown of Passivity and Consequent Pitting Initiation

With the above background regarding the various theories related to the passive film, the factors leading to local breakdown of passivity should be investigated. It has been claimed that pitting corrosion occurs only on metals whose chemical affinity for halogens is less than that for oxygen[22], and it has frequently been argued that the halide ions enter the growing anodic oxide lattice more easily than oxygen and thus causes instability of the oxide[18]. It has also been claimed by Kolotyrkin[22] despite evidenced to the contrary[50] (by Hoar, Mears and Rothwell) that chlorine is more easily adsorbed on the metal surface which is supposed to carry a layer of adsorbed oxygen, and that once there, it favours hydration rather than oxidation of the metal ions, and therefore favours solution rather than protective film formation. A combination model of adsorbed film and oxide layer has been proposed by Andreeva.[51]

Numerous models of film penetration have been proposed. Hoar[19] has argued that anions of strong acids promote pitting because the presence at anodic points in the film prevent a rise in pH, and hence prevents the production of blocking precipitates that promote passivity. The limitation of this model is that it presupposes the existence of anodic points in the film and is thus a better model for explaining the continuation of pitting attack rather than for initiating it. The

same criticism may be made of a model of Hoar and Evans,[52] which argues that halide ions promote attack on weak points in the film which allow easy escape of cations. In the subsequent paper[50] Hoar et al have adopted the view that the halide ion initially adsorbes on the film surface and then diffuses through the oxide film under the influence of the anodic potential. It reacts, in course of this diffusion, with any cations that may be diffusing outwards and thus produces a contaminated film which is a better ionic conductor than the original. A similar model has been proposed by Nielsen[53]. It is argued that this promotes further inward diffusion of halide ions, and that it may (??) further facilitate outward diffusion of cation - breakdown of the film now occurs in the contaminated area, which may now consist of material soluble in the electrolyte and pitting results. The localised nature of breakdown is claimed to result from preferential halide penetration at disarranged points in the oxide film lattice, perhaps corresponding to grain boundaries, impurity zones, segregations, dislocations or other disarrayed zones of the metals.

(ii) Potential Across the Double Layer

When an electronic conductor is in contact with an electrolytic solution, a case which is always present in aqueous corrosion studies, a compact electricaldouble layer is formed consisting of a layer of electrons or holes on one side (the solution side) and a layer of ions adsorbed at the interface (on the metallic side). The diffuse double layer which is on the solution side consists of an excess concentration of ions of one sign and a defect of ions of opposite sign, as compared

to their respective concentration in the bulk solution. At the interface there may also be a layer of adsorbed neutral atoms or molecules including water, which may or may not be oriented. A schematic representation of the double layer is given in Figure 5. It has been estimated that a potential of 10^7 volts exists across the double layer.

Assuming that a passivated layer on the surface of stainless steel consists of a layer of weakly bonded oxygen ions, physically adsorbed on the surface and held by Van Der Waal forces, then to analyse a situation where such a passivated layer is encountered with a corrosion solution the following factors would come into the picture: -

(i) Surface Diffusivity of Anions

(ii) The effect of potential across the double layer on the diffusion characteristics of the adsorbing species.

(iii) The effect of the hetrogenity of the metallic surface, due to the presence of alloying elements such as Molybdenum, silicon, etc., on the binding forces of the anions.

(iv) The stability of the adsorbed layer with respect to variations in external parameters, such as pressure, temperature and concentration of electrolyte.

The Case when No Passivating Layer is Present.

In this case anions have to cross the double layer and before they become adsorbed species they must diffuse to dissolving sites. Whether or not surface diffusion can be the rate controlling step depends upon the ratio of the mean free path of diffusion X_D to the

distance between the mean free path between the dissolving sites X_0.

$$D_S = a^2 \nu \exp\left(-\frac{U_s}{RT}\right)$$

where D_S = Surface diffusivity

a = distance of surface atoms from one another

ν = frequency factor

U_s = Activation Energy

Assuming that the dissolution sites are the kinks on the steps of the surface and that diffusion along the steps is very rapid compared to the diffusion along the plane surface, then X_0 represents the distance between dissolution steps. Let γ_e be the edge free energy of a step. It has been shown, by Fleischmann and Thirsk, that there is a parabolic dependence of γ_e upon the electrode potential, E.

$$\gamma_e = \left[\gamma_e\right]_o - \frac{c}{2} (E \pm \eta)^2$$

The case when a Passivating Layer is present

When a passivating layer is present, i.e., when an adsorbed layer of oxygen is present on the surface, the relationship between surface excess, surface tension and interfacial charge density has been derived by Grahme and Whitney[66] as:

$$d\gamma = qd(\psi^{\beta} - \psi^{\alpha}) - \sum \Gamma_2 \, d\mu_2$$

where γ = surface tension, $(\psi^{\beta} - \psi^{\alpha})$ = P.D. across the interface

Γ_2 = surface excess, μ_2 = chemical potential of the adsorbed species

or

$$k(\psi^{\beta} - \psi^{\alpha}) = d\gamma + \sum \Gamma_i \, d\mu_i$$

Thus, the presence of adsorbed oxygen increases the potential across the double layer. In such a case, to bring an anion from the solution to the surface (say, a chlorine ion) greater amounts of work will have to be done. This will amount to increasing the resistance to dissolution - rendering the metal or alloy more corrosion resistant.

(g) Methods to Determine Susceptibility to Pitting Corrosion of Austenitic Stainless Steels.

When testing for susceptibility to pitting corrosion the critical consideration is not corrosion rate, as it is a localised form of corrosion, but rather the conditions under which pitting corrosion may or may not occur. Under pitting corrosion conditions the material may be penetrated and rendered useless even if there is a low corrosion rate indicated by the conventional weight-loss tests.

I POTENTIOSTATIC METHOD OF DEFINING THE PITTING RANGE

Pitting corrosion can occur only within a definite range of potential lying within the passive range. Limits of pitting potential may be investigated most reliably by a potentiostatic point technique, in which the sample is left with a constant potential in the corrosion environment and is examined after certain periods of time, say 2 hours, 6 hours, 12 hours, 24 hours, etc., for formation of pits. Then the test is repeated for a different sample at a different potential, say in steps of 25 mv. In this manner transition in pitting range is investigated and accurate statements regarding limits of pitting range can be made. Brauns, Schwenk and others,[11,27] carried out experiments in this field in the above manner.

II "SQUARE-DROP" TEST [10,28]

The "square-drop" test was sucessfully used by Mears and Brown[10], and Evans and Mears[28], for determining pit-initiation in iron and stainless steels. In this method sample was made to corrode in KCℓ solutions under oxygen-nitrogen mixtures - the probability of attack was found to diminish and the rate of corrosion increased with oxygen concentration.

III ELECTROLYTIC METHODS

(A) Method of Donker and Dengg[29]

Donken and Dengg applied an external E. m. f. to a cell consisting of iron anode and silver cathode in solutions of various salts.

A breakdown potential was reached at which there was a large increase in current through the cell. The increase in cell current was caused by dissolution of iron. This technique was used by Uhlig[2] and in modified form by Mahla and Nielsen[30] for study of the passivity of stainless steels.

(B) Electrolytic Method as used by Streicher[17]

The drawback of the method described in Part A was that most of the attack took place at the edges of the specimen. A modified apparatus was used by Streicher to determine the Electrode potential for initiating pitting for a small area of stainless steel. A 25 sq. cm. surface area was tested and the primary measurement was the number of points for film breakdown, i.e. no. of pits initiated rather than potential at breakdown. The results obtained by Streicher are outlined below:

(i) <u>At Constant Current Density</u> no. of pits per square cm. does not vary with time;

(ii) <u>At Constant Area</u> Linear relationship between pitting density was obtained. As expected, the slope of the curve for pickled sample was greater than for the one in pickled and passivated condition.

IV TWIN-PROBE METHOD

Danilov and Rosenfeld[7] devised a "twin-probe" method which allows the measurement of potential difference -- ΔV -- in any direction between two points in an electrolyte with the aid of two non-polarised differential electrodes. Data are provided by them for the variation

with time of the electrical field strength and current density of pit-generating current for 5-15 minutes, 20-60 minutes, and for stable operating pits using 0.05 M$FeNH_4(SO_4)_2 \cdot 12\ H_2O$ + 1M$NH_4C\ell$. The findings obtained are:

(i) a great number of pits originate together, after which no more appear;

(ii) rates of metallic dissolution are similar for all pits initially, but subsequently differ markedly -- in some pits the process stops, whereas in others, the pits continue to generate current. The current flow varies parabolically with time;

(iii) anode current characteristics suggest that a process occurs in a relatively closed area under the film -- the size distribution is associated with metal passivation in the pits and with the gradual stopping of dissolution;

(iv) anode current density in the pits were estimated to be 120 mA/cm^2 and the associated cathode current density 0.4-0.6 mA/cm^2;

(v) the pitting inhibition mechanism has been related to the ability of the anion to be adsorbed and to displace corrosive ions.

V ARTIFICIAL PIT METHOD

In the method used by P. M. Aziz[33] radioactive ions were introduced in the solution after pitting of the sample had proceeded for a pre-determined length of time. The tracer -- radioactive Co or Pb -- was then permitted to plate out on the local cathodes, and after washing and drying radiographs of the surface was prepared. Results indicate, that the pits were surrounded by annular rings of

passive surface which prevent lateral expansion of corrosive attack. This method was used for Aluminum, but could as well be used for Austenitic stainless steels.

PART B INTERGRANULAR CORROSION OF AUSTENITIC STAINLESS STEELS

Introduction

The phenomenon of Intergranular corrosion of Austenitic stainless steels, though well appreciated by its detrimental consequences, is not yet fully explained from a morphological and Kinetic standpoint.

Austenitic stainless steels have excellent corrosion resistance properties when properly heat treated and used at temperatures where sensitisation Kinetics (i.e. amount and rate of carbide precipitation) is slow. It has been observed that these steels, when slowly cooled through the temperature range of 400°C-750°C or after solution quenching from higher temperatures are again held in the above temperature range, lose their corrosion resistance properties. This has generally been attributed to the precipitation of chromium carbides, usually $(FeCr)_{23}C_6$ or Cr_3C_3 or other complex carbides at the grain boundaries. This high chromium content of the carbide will take place from a thin Zone of the matrix along the grain-boundaries. (The diffusion processes, which take place during the course of this precipitation, is explained by means of a simple mathematical model in Appendix I.) If the chromium content in the depleted Zone falls below a certain critical value, the Zone loses its corrosion resistance and the material is said to be sensitised or sensitive to Intergranular attack. The corrosion re-

sistance properties may, however, be restored by further subjecting the steel to solution treatment followed by rapid quenching.

The susceptibility to Intergranular Corrosion in Austenitic Stainless Steels is minimised by the following:

(i) using steels with very low Carbon -- less than 0.03%. Lower the carbon content, lower will be the carbon available for the formation of carbides and, hence, lower will be the sensitising susceptibility;

(ii) use of "Stabilised Steels" -- by the addition of Titanium and Niobium, in amounts varying from seven to ten times the carbon content, the preferential formation of carbides of these elements will take place. (This is explained on the basis of lower free energy of formation of TiC which is -56.5 Kcal as compared to -16.7 Kcal at 298°K for $Cr_{23}C_6$.) This means that by the addition of Titanium, the free chromium content of the steel is practically left unaltered even when held in the sensitisation range.

The presence of Molybdenum in the Steel (AISI 316) also helps to reduce the corrosion Kinetics in the sensitisation range. This can be explained on the basis of a thermodynamic -- cum -- Kinetic model, to be discussed later, which has been proposed in the course of the present work.

(a) Theories of "Formation of Depleted Zone" and Correlation with Intergranular Corrosion

The model of the "chromium-depleted Zone" which has been presented above, has been subject to critical review from time to time. Using

the electron microanalyser several workers -- Hopkinson and Caroll[34], Weaver[35] and Plateau[36] were unable to find any depleted Zone, whereas others, Philbert[37], Pomey[38] and Fleetwood[39] did find such a Zone. Obviously, the difficulty in observing the depleted Zone is caused by its very small thickness and not due to the questionable nature of its existence. In a research project sponsored by "JERNKONTORET" the effect was greatly exaggerated by using unusually high carbon content and temperature, and good evidence of the depleted Zone was obtained[40]. In order to circumvent the difficulty in observing the depleted Zone under more practical conditions, the following model was proposed by Stawstrom and Hillert[41].

Model of Stawstrom and Hillert

Although the carbide precipitation occurs at the grain boundary, its geometry is very complicated. It was assumed that a grain boundary film of even thickness forms and, thus, the diffusion in the film is essentially one-dimensional. At low temperatures, this approximation yields reasonably correct results for the diffusion in the matrix towards grain boundaries, since the rapid grain-boundary diffusion will allow equilibrium to be established along the grain boundaries between the carbide particles and all the grain boundary area of the matrix. Figures 6a and b show the expected concentration profile during precipitation of grain boundary carbide. The thickness of the chromium-depleted Zone, l, is given by the relation,

$$\tfrac{1}{2}l = \sqrt{2Dt}$$

where D = diffusion coefficient of chromium in Austenite and t is the time. Since diffusivity of carbon is much greater than that of chromium, carbon can diffuse from much larger distances. Thus,

carbon activity in the whole material at all times may be assumed to be uniform. The concentration profiles of carbon during precipitation of grain boundary carbide is shown in Figure 6.

The presence of nickel in Austenitic Stainless Steels has several effects:

(i) it prevents the α-phase from forming;

(ii) it affects the activity coefficient of carbon in the Austenite;

(iii) it distributes itself in a characteristic manner between the carbide and austenite.

Only the first two effects have been taken into account, and the third has been ignored. (Although Philbert[37] points out that the carbide will contain only half as much nickel as the average steel content. However, Hillert et al feel that this effect is only of minor importance as compared with the diffusion of chromium to the carbide.)

Based upon this model, the following conclusions can be drawn:

(i) the calculated annealing time for developing a chromium-depleted Zone, agrees will with the experimental annealing time that makes the steel sensitive to Intergranular Corrosion;

(ii) on prolonged annealing the carbide film will continue to grow. As the carbon content of the austenite decreases, the carbon activity of the steel will decrease, and this will, in time, allow the chromium content of the depleted Zone to increase;

(iii) the annealing time for this so-called phenomenon of "self-healing" varies quadratically with grain size; and,

(iv) the authors claim that the calculated rate of decrease of carbon content in the austenite matrix agrees well with the experimental data.

Model of Aust, Armijo, Koch and Westbrook [42,43,44]

A simple model is presented in which it is proposed that the intergranular corrosion of Austenitic Stainless Steels is associated with the presence of continuous grain boundary paths of either a second phase or solute segregated regions. It is suggested that the Intergranular Corrosion rate could be markedly reduced by the formation of a DISCONTINUOUS SECOND PHASE at the grain boundary (rather than a continuous one) if it would incorporate a major part of the segregating solute drained from the grain boundary region. It is clained that the results of corrosion tests and Electron Microscopic studies of AISI 304 steel after various heat treatments provide support to this model.

The results obtained by these workers contradict, to a considerable extent, the classical model of Chromium-depletion theory of Intergranular Corrosion. According to the chromium depletion theory, the beneficial effects of stabilisation heat treatments on corrosion of Austenitic stainless steels is due to the diffusion of chromium into the Cr-depleted Zones adjacent to the precipitated carbides. However, it was experimentally seen that when type 304 is slowly cooled from 1300°C to 900°C at about 2°C/min, held at 900°C for 1 hour, and quenched, a high rate of attack is still observed. In other words, at the same annealing temperature and time where chromium diffusion is thought to replenish chromium-depleted regions, poor corrosion resistance is found. This is due to observed continuous carbides present at the grain boundaries. This result is in agreement with the present model, but not with the chromium-depletion concept.

The fact that severe intergranular attack is also observed, at times, in the absence of any carbide precipitate at the grain boundary, also indicates the limitation of the "depletion theory" for intergranular corrosion.

Model of Tedman and Vermilyea[54]

The above workers in a recent paper, have tried to build up a thermodynamic model for calculating the Cr-C-$Cr_{23}C_6$ equilibria in and near grain boundaries in order to determine the chromium content in the vicinity of the carbide particles.

$$23Cr + 6C \rightleftharpoons Cr_{23}C_6$$

$$\text{Equilibrium Constant, } K = \frac{1}{(\gamma_{Cr}X_{Cr})^{23}(\gamma_C X_C)^6}$$

where γ is the activity coefficient and

X is the mole-fraction.

Unit activity has been assumed for the carbide. Data for free Energy of formation are available[55] and, hence, K may be determined. In order to determine X_{Cr}, it is, then, only necessary to calculate activity coefficients for carbon and chromium. This has been done using the Wagner Analysis for Calculations of the Carbon Activity Coefficients -- shown in Appendix II. In a similar manner, γ_{Cr} is calculated.

The calculations show that the equilibrium chromium content is a strong function of the temperature and the carbon and alloy content of the steel. It is inferred from the analysis that the variations in the susceptibility to Intergranular attack are determined primarily by the changes in the equilibrium chromium content near the carbides and secondly by changes in the number and distribution of particles.

For instance, it is claimed, that above 800°C, the chromium passivity and the alloy is immune not because of the absence of carbides, but because chromium depletion is not severe.

Limitations of the Above Model

(i) The application of Wagner's analysis for calculating the activity coefficient of carbon and chromium based on the assumption that the alloy is a "dilute" one is questionable. For, the validity of such an application to Austenitic stainless steels, which contains more than 25% of alloying elements, on the premise that Henryan behaviour will still hold, is highly debatable.

(ii) Even if such analysis is made, the calculations leading to the determination of γ_{Cr} based upon the assumption that $X_C \frac{\partial \ln \gamma_{Cr}}{\partial X_C}$ can be ignored is not totally valid. For, the manner in which carbon content affects the activity coefficient of chromium is not known, and, thus, even if X_C may be small, the product of the two terms may not be negligible.

(iii) The above model does not indicate, even in a qualitative manner, how the presence of certain alloying elements such as Molybdenum, exert a beneficial effect upon the corrosion properties. To explain this, a simple model has been proposed, in course of the present work, which will be discussed later.

(b) Factors Effecting Inter-Granular Corrosion of Austenitic Stainless Steels

I Chemical Composition

(a) Carbon The lower the carbon content, lower is the susceptibility

to Intergranular corrosion. This becomes self-evident when it is realised that this is related to the lower probability of formation of chromium carbide at the grain boundaries, either as descrete particles or as continuous networks[1,14].

(b) Stabilising Elements Titanium and Niobium

As already pointed, these elements "stabilise" the steels due to their preferential affinity towards carbon as compared to that of chromium. Thus, grades AISI 321, 347, 356 have better corrosion resistance properties than other austenitic grades in the sensitising ranges of temperature.

(c) Molybdenum The presence of Molybdenum in Austenitic Stainless Steels has a beneficial effect upon the localised corrosion resistance properties, particularly in the sensitising range of temperature. No satisfactory theoretical explanation has been provided for this -- the argument which has been given is that is improves the passivating ability of the steel. A model is presented, based upon thermodynamic and Kinetic factors, which tries to explain this behaviour. (This is explained in the discussion of Experimental results.)

II Heat Treatment

This aspect was discussed while considering the various models for "Depleted Zone Theory". The effect of heat treatment may best be summarised by saying that any heat treatment which induces the formation of continuous network of carbide along the grain boundaries render it susceptible to Intergranular attack.

The chemical composition and thermal treatment of the austenitic steel should be so chosen that there is no possibility of formation of continuous carbide network along the grain boundaries in order that the corrosion resistance properties of the steel are not impaired.

(c) Methods of Detecting "Intergranular Attack"

I Optical Micrography The simplest and the most conventional method to study the damage done by intergranular attack is to etch the specimen (after suitable polishing) by chemical reagents such as alcoholic Ferric Chloride, Murakamis' reagent or by electrolytic means. The attack on the grain boundary, if any, is easily revealed under high magnification microscopes.

II Chemical Tests The tests depend upon the use of some reagent which exerts a specific action on the carbides at the grain boundary which, if present, causes susceptibility. As for example, Hatfield's method[60] of using Copper sulphate solution acidified with sulphuric acid, which attacks the impoverished network, if present, so that grains of a susceptible steel become dislodged is very effective. Given time, the whole specimen may fall to powder, each grain representing a grain of the alloy.

But, the interpretations of these chemical tests should be done with caution. A sample which may, for example, fail in a test in hot nitric acid, may withstand the test in acid Copper Sulphate solution. For a critical appreciation of the relative merits of these tests, a reference is made to the work of H. T. Shirley and J. E. Truman[60].

III Electron Microscopy Armijo and Aust[42-44], Hopkinson[34], Philbert[37], and others have used electron micro-photographs to great advantage in correlating the effect of various heat treatments on the Intergranular corrosion of 18-8 austenitic stainless steel. Either the CARBON-REPLICA technique (two-stage replicas) or the transmission electron micrograph may be studied. Transmission electron micrographs, after being subjected to thermal treatments in the sensitising range, from thinned foils of the samples, give excellent indication whether the carbides have formed a continuous network or have precipitated as descrete particles.

IV Electron Micro-Probe Analyser Plateau[36], Pomey[38], Weaver[35] and Baumel[38] have used the electron micro-probe analyser to study the existence of the "depleted zone". As pointed out earlier, the difficulty in observing the depleted zone is due to its very small thickness (of the order of 200-500 Å) in the conventional austenitic stainless steels, particularly those with low carbon contents or those having Mo or stabilising elements. Hence, apparently contradictory results have been obtained. Whereas, Baumel[38], Strauss and Hopkinson could not identify the presence of the depleted zone by the microprobe, Philbert[37], Pomey and Fleetwood did identify the zone.

V Potentiostatic Methods The precise environmental conditions necessary for the intergranular corrosion of Austenitic stainless steels have been determined by potentiostatic methods by France and Greene[61]. They conclude by saying that the intergranular corrosion of these steels occur in limited potential range.

They use their results to predict the intergranular failure tendencies of the steels in various sulphuric acid environments. They show that sensitised steels may be used in many media without the occurence of intergranular attack.

It has been argued that the presence of chromium depleted Zone is a necessary but not a sufficient condition for intergranular attack. Many environments do not selectively attack the grain-boundaries and for these media, the use of costly preventives (such as, inhibitors) is unnecessary.

However, Streicher[62] has questioned the validity of the above findings in so far as the time factor in the above potentiostatic studies have been ignored. For example, France and Greene state that, in $1NH_2SO_4$ at 90°C, no Intergranular attack on austenitic stainless steel specimens are observed whose potential was held at 0.60 V (S. C. E.). It was found by Streicher that under the above conditions, no perceptible attack occured up to about 30 hours of exposure, but when the length of attack was steadily increased to, say, 330 hours, a period not uncommon in industrual use, attacks of considerable intensity did occur. Similar conclusions have been arrived at, by Osazawa Bohenkamp and Engell.[62] On the basis of potentiostatic tests on sensitised stainless steels in $2NH_2SO_4$ at 90°C, they report on the basis of current measurements and metallographic examination that there is an intergranular attack over the entire active and passive range of potentials.

Thus, the potentiostatic methods of France and Greene provide reliable information for only short testing times used by them. If their data are used for predicting resistance of sensitised stainless steels to sulphuric acid attacks for

periods approaching industrial conditions quite contradictory results would be obtained.

(d) Correlation Between Pitting and Intergranular Corrosion

No specific attempt has been made to correlate these two forms of localised corrosion in austenitic stainless steels by workers who have studied these two phenomena individually. However, on the basis of results obtained, the following correlations can be made:

(i) Effect of Alloying Elements

Carbon Lower the carbon content, lower is the rate of both intergranular and pitting attack[14,17].

Nickel, Chromium, Molybdenum An increase in the alloying percentage of these elements improve the resistance to both pitting and intergranular attack[1,14,17]. The positive effect of these elements is due to the formation of a more stable, homogeneous austenitic structure. Further, they aid in the formation of a more resistant passive film. (This has been discussed under the heading "Role of Passive Films".)

Silicon When Silicon is present in Austenitic Stainless Steels with Mo, resistance to both pitting and intergranular attack is increased[14,65].

Titanium and Niobium These have opposite effects on intergranular and pitting corrosion. Both these elements are added as stabilisers to improve the intergranular corrosion resistance properties. But, the addition of these were found to have detrimental effect upon resistance to pitting corrosion[14].

(ii) Locus of Attack Tomashov[14] and Streicher[17] suggest that pitting occurs mainly at grain boundary -- which, if valid, should strongly establish ties between the two forms of localised corrosion. However, Danilov and Rosenfeld[7] show that no such preference exists for initiation of pits.

As far as the physical structure and chemical composition are concerned, the grain boundaries differ from the bulk of the grain and precipitation of secondary phases are liable to occur at the grain boundary. For this reason, the passive state at the grain boundaries is lower in protective properties than in the grain proper. Pitting may be due to the precipitation of secondary phases resulting in heterogeneity of metal composition. In the presence of ferritic inclusions, austenitic steels become increasingly susceptible to pitting corrosion. Thus, the elements which tend to cause heterogeneities in the structure decrease its resistance to localised corrosion -- whether pitting or intergranular.

(iii) Effect of Heat-Treatment The effect of sensitising on pitting corrosion has not been conclusively established. Tomashov[14] shows, though not definitely, that heating in the sensitisation range strongly enhances the susceptibility to pitting. But, France and Greene[61] do not agree that such correlations hold good in the generalised way.

CHAPTER II

EXPERIMENTAL PROCEDURE

The experimental work undertaken, was done in order to study the following aspects of localised corrosion of Austenitic Stainless Steels:

(A) comparison of localised corrosion behaviour of 316L in Solution Quenched and sensitised condition;

(B) to demonstrate the effect of Molybdenum in improving localised corrosion behaviour by studying the difference between 316L and 304L;

(C) to demonstrate the effect of carbon by comparing 316L and 316 and 304L vs. 304;

(D) to demonstrate the effect of carbide morphology on the corrosion resistance of Austenitic Stainless Steels in sensitised condition;

(E) to study the role of passive films on corrosion resistance;

(F) to investigate the corrosion behaviour of Austenitic Stainless Steels in Kolene Bath -- a highly basic solution used industrially before pickling of Stainless Steels.

The tools for examination for the above study were:

(a) optical microscope;

(b) Scanning Electron Microscope;

(c) Electron Microscope using Carbide Extraction replica technique;

(d) a new method was improvised using the plastic replica study on Scanning Electron Microscope.

(A) Material

The grades of Austenitic Stainless Steels used for experimental analysis are given in Table I.

(B) Heat Treatment

The heat treatment cycles of the grades used for corrosion studies may be summarised as follows:

Heat at 1300°C for ½ hour ⟶ water quench ⟶ clean the surface by immersing in 10% Sulphuric Acid for 10 minutes ⟶ sensitise at 650°C for times varying from 15 minutes to 72 hours ⟶ Furnace Cool ⟶ clean in H_2SO_4 for 10 minutes ⟶ Passivate in 2% HNO_3 for 5 minutes.

The solution-treatment temperature used commercially is 1100°C. The unusually high temperature of 1300°C for solution-treatment was used to obtain large Austenitic grain size to facilitate consequent corrosion behaviour with respect to grain boundaries and grain interior.

The samples prepared for the heat-treatment and subsequent corrosion studies were approximately of the size 25 mm x 10 mm. After the heat-treatment, the samples were polished mechanically until 1 micron diamond.

(C) Corrosion Testing

(i) The solution in which the corrosion studies were carried out was Alcoholic Ferric Chloride of the following composition:

TABLE I

	GRADE	COMPOSITION (WT. %)								REMARKS
		C	Mn	P	S	Si	Cr	Ni	Mo	
I	316 ELC	.026	1.45	.008	.009	.32	18.42	11.65	2.59	Vacuum melted
II	304 ELC	.028	1.54	.013	.009	.37	17.90	8.43	0.25	Vacuum melted
III	316	.055	1.58	.024	.015	.44	17.11	12.37	2.65	Commercially melted
IV	304	.060	1.56	.025	.015	.37	18.32	9.38	0.33	Commercially melted
V	304	0.070	1.60	.028	.012	.23	18.61	8.34	0.30	Commercially melted

(A) Extra Low Carbonspecification -- where maximum carbon permissible is 0.030%.

(B) Vacuum melted grades were samples supplied by Allegheny Ludlum Co. and the Commercially melted grades were supplied by the Atlas Steels Co.

(C) Samples I and II were supplied as Hot-rolled sheets and those of III, IV, V were Cold-rolled.

$FeC\ell_3$ = 20 gms., Ethanol = 384 c.c., $HC\ell$ = 8 c.c., $NaC\ell$ = 5 gms.

This solution served a double purpose:

(a) revealing grain-structure for metallographic studies;

(b) to demonstrate the effect of aggressive chlorine ions on localised corrosion for the purpose of standardisation, sufficient bulk of the stock solution was prepared and 50 c.c. of the solution was used for each of the studies. Continuous stirring was done by a glass stirrer attached to an electric motor.

The samples which were tested after the particular thermal treatments are given in Table I. The optical micrographs obtained are given in the following Chapter.

(ii) Corrosion Behaviour in "Kolene"

Industrial Problem

"Kolene" is a patented mixture which is basic in nature. Its approximate composition is given below:

NaOH: 61%, $NaNO_3$: 15%, $NaCrO_3$: 10%, $NaCO_3$: 10%

Stainless Steel sheets after being hot-rolled and annealed are passed through the pickling line in the following sequence:

Hot Rolled Sheets ⟶ Annealed in Roller Hearth Furnace (1100°C for 20 mts -- 30 mts) ⟶ Descaling Salt (Kolene) ⟶ rinse in water 480°C (15-20 minutes) ⟶ 10-12% Sulphuric Acid (75/80°C -- 8-12 mts.) ⟶ Rinse ⟶ 2% HNO_3 + 2% HF (35°C -- 5 mts) ⟶ Rinse ⟶ 2% HNO_3 (Passivation -- 35°C -- 5-7 mts.) ⟶ Forwarded for Cold Rolling.

The descaling salt loosens the surface scale by combined thermo-chemical effect. The scale and the parent matrix have different coefficient of thermal expansion and, thus, due to differential expansion in the hot bath, the scale cracks due to resulting stresses. This facilitates the scale removal in the subsequent sulphuric acid tank and also reduces the time for pickling by 25-30%.

But, the problem faced under industrial conditions is that, at times, the surface of the sheets display a pitted rough appearance after the treatment in the Kolene Bath. The solutions may be found by investigating the factors which may come in the picture when the Austenitic Steels come in contact in an alkaline medium.

The industrial condition was simulated by setting up a salt bath and heating the "Kolene" salt at 480°C at which the salt is molten and viscous. The steel sample (25 mm x 10 mm x 2 mm) was introduced by suspending with a Steel wire and clamp.

The samples were introduced in the bath in both solution quenched and sensitised condition. The nature of attack in this basic solution was studied and compared with the local corrosion behaviour in the chloride solution.

II (d) Electron-Microscope Techniques

For the examination of localised corrosion processes, Electron Microscopy was used, with great advantage. Three different techniques were adopted.

(i) Scanning Electron Microscope

The study of sensitisation process was very effectively demonstrated by Scanning electron micrographs. This was particularly helpful in establishing the locus of pit initiation in sensitised condition as is shown in micrographs, Figures 10, 12 and 13.

(ii) Carbide Extraction Replica Technique

In order to study the morphological characteristics of carbides precipitated during the sensitisation process, Extraction Replica Technique was used. The sequence of preparation is outlined below:

(a) the specimen surface was coated with a layer of thick plastic solution (Parlodion was used). It was allowed to dry for a period of 5-6 hours;

(b) after it was dry, the plastic layer was stripped taking due precautions. A corner of the film was lifted by laboratory tweezers. The outline of the film was marked by a sharp cutting edge. Then, by gentle application of pressure, the film was stripped;

(c) it was placed on a glass slide, and the ends were secured by adhesive cellotape;

(d) the plastic film was shadowed with Gold-Palladium (shadowing helped in improving the contrast between the precipitates and the surrounding matrix). The angle of shadowing was 10-15° from horizontal;

(e) a thin film of carbon was deposited on the plastic film -- the thickness of this film being 200 Å;

(f) the surface of the deposited film was cut in small square grids suitable for examination on the electron microscope. These were carefully placed on the wire-mesh grids, kept on three filter papers inside a covered glass container. A few drops of Iso-amyl Acetate were added to dissolve the initial plastic film leaving behind the extracted carbides on the carbon substrate. This was left overnight for complete dissolution of plastic;

(g) the carbides, thus left after the above sequence of operation, were examined under suitable magnification.

(iii) Study of Plastic Replicas by Scanning Electron Microscopy

This method was improvised to study sensitisation behaviour after prolonged sensitisation time. The practical difficulty encountered in studying carbide morphology by the second method viz two-stage carbide extraction replica technique was that the size of carbides obtained after more than 24 hours at sensitisation temperature, was so big that high magnification study by electron microscope was not possible. Moreover, this method of studying plastic replicas with S. E. M. was more rapid and less liable to setbacks due to improper conditions of carbon deposition and subsequent dissolution.

CHAPTER III

RESULTS

The results of the corrosion studies as observed by Optical and Electron Microscopy are given in Figures 7 to 51. The observations may be catagorised under the following divisions:

Part A

316L -- EFFECT OF SENSITISATION ON LOCALISED CORROSION BEHAVIOUR

(i) Distribution of Sites of Attack

Figures 7 and 17a show that in the solution-quenched condition, the attack is of a uniform nature -- there being no preferred sites for initiation of attack. The uniform distribution of pits in the solution-quenched condition, both in the interior of the matrix and near the grain boundaries is due to the fact that local anodes and cathodes do not exist due to uniform distribution of chromium throughout the matrix. But, as the steel is sensitised at 650°C for progressively increasing amount of time, the attack becomes preferentially localised to the grain boundaries and incoherent twin-boundaries. The preferential attack along the incoherent twin-boundaries is shown in optical micrograph (Figure 11) and the S. E. M. (Figure 12). The theoretical reasons for the preferential attack along the grain boundary and incoherent twin-boundaries has been already discussed in Chapter I. Figure 10 shows that the pit initiates near the grain boundary,

possibly in the depleted zone and grows towards the interior.

(ii) Intensity of Attack

Longer the time of sensitisation, greater is the severity of localised attack along the grain boundaries. This becomes evident by comparing Figures 10 (time of sensitisation -- 24 hours) and 13 (time of sensitisation -- 96 hours).

(iii) Time of Pit Initiation

The method utilised is a simple one -- after being subjected to attack in the alcoholic ferric chloride solution-periodic optical micrographic examinations were made to observe the initiation of localised attack. The results for 316L, in active and passive conditions, after progressive increase in sensitisation time, are given in Table II.

Remarks

(a) In the "Passive" condition, the steel surface has been given the treatment in 2% HNO_3 for 5 minutes, whereas in the "Active" condition, this treatment has not been given.

(b) The quantitative significance of the Pit initiation time cannot be overemphasized, for this will, to a great extent, depend upon surface conditions such as adsorbed impurities, surface heterogeneities, emerging dislocations, and other surface imperfections. But, a definite qualitative conclusion which can be drawn is that, in the passive condition, resistance to attack in a chloride medium is more than that in the active condition. The theoretical aspects of this are discussed in Chapter IV.

TABLE II

TIME OF PIT INITIATION AS A FUNCTION OF SENSITISATION TIME

	TIME OF SENSITISATION	TIME TO INITIATE PIT (MINUTES)	
		ACTIVE	PASSIVE
i)	Solution-Quenched (Not Sensitised)	180	205
ii)	2 hours	135	150
iii)	4 hours	105	115
iv)	24 hours	60	75
v)	48 hours	50	60
vi)	96 hours	35	50

(c) But, once the localised attack has started, the morphological characteristics of the surface attack in both the active and the passive conditions are the same. This is indicated by comparing Figures 7 and 16 (solution-quenched, active vs. passive conditions, Figures 9a and 9b (4 hours sensitisation, active vs. passive) and Figures 17a and 17b (316, solution quenched, active vs. passive)).

Part B

COMPARISON OF CORROSION BEHAVIOUR OF 316L VS 316 AND 304L VS 304 TO SHOW THE EFFECT OF CARBON

The intensity of localised attack is lower for the "EXTRA LOW CARBON" grades as compared with the normal carbon austenitic grades. 316L and 304L exhibit better resistance to localised attack as compared with 316 and 304, respectively. By comparing Figures 7 and 17a, it can be pointed out that 316L has fewer number of sites of attack in the solution quenched condition as compared with those of 316. Similarly, by comparing Figures 13 and 22, it becomes evident that in the sensitised condition; for the same period of sensitisation, the attack is more severe for 316 as compared to 316L.

Further, in the commercial grades, higher the percentage of carbon, more severe is the nature of attack, both in solution quenched and sensitised condition. Thus, the two commercial grades of 304, one with 0.06%C and the other with 0.07%C, show that the severity of attack is more with higher percentage of carbon. This can be shown by comparing Figures 28 and 29 (sensitisation period

24 hours) and Figures 30 and 31 (sensitisation period 48 hours).

However, it should be pointed out that the nature of attack as regards the distribution of sites is independent of the carbon concentration. In all the grades, in the solution-quenched condition, the attack takes place more or less uniformly throughout the matrix; and, then, with progressive increase in the time of sensitisation, the attack becomes more and more localised along the grain boundaries and along the incoherent twin boundaries.

Figure 26 shows that the attack initiates near the grain boundaries in the sensitised condition and propogates towards the interior. Figure 22 indicates how severe is the attack in the so-called "depleted zone" after prolonged period of attack -- 96 hours. Further, in all of the sensitised specimens, there is observed a preferential attack along the incoherent twin boundaries in addition to the grain boundaries.

Part C

CORROSION BEHAVIOUR IN "KOLENE" BATH

The solution quenched sample after a period of 15 minutes treatment in the "Kolene" solution, gave a pitted appearance as indicated by Figure 32. When the period of treatment was increased to 30 minutes, the surface became very rough and patchy. Figure 33 shows the optical micrograph in this condition. The globular patterns obtained is due to the particles of salt con-

stituents of "Kolene" being firmly attached to the resulting pits. The pits produced are very deep (about 4 microns) as measured by Interferometry -- Figure 34). Under such conditions of pit depth and rough surface appearance in industrial practice, the stainless steel sheets are rendered unacceptable. Thus, the period of treatment should not exceed 15 minutes.

Part D

CARBIDE MORPHOLOGY

The effect of the sensitisation treatment upon the carbide morphology as observed by extraction replica techniques has been tabulated in Table III.

It is of significant interest to note the changes in shape and distribution of the carbide particles with progressive increase in the time of sensitisation. In the Molybdenum -- bearing grade AISI 316, the dendritic configuration of these particles persists until about 4 hours at the sensitisation temperature (Figures 35, 36 and 37). During this time, the dendritic arms thicken and, subsequently, fragment. After about 2 hours, some equiaxed carbide particles are also observed. In contrast with this, the AISI 304 (Figure 39) grade exhibits a much more dramatic change in the shape of the carbides precipitated. Until about $\frac{1}{2}$ hour of sensitisation time, the shape of carbides are dendritic as in the case of 316 (Figures 43 and 44), but, after this, the particles abruptly assume an equiaxed shape (Figures 46 and 47). The consequence of such changes are discussed in Chapter IV D.

TABLE III

TEMP. OF SOLUTION TREATMENT 1300°C

TIME OF SOLUTION TREATMENT ½ HR.

TEMP. OF SENSITISATION 650°C

NATURE AND DISTRIBUTION OF CARBIDE PRECIPITATES

TIME OF SENSITISATION	GRADE 304	FIG. NO.	GRADE 316	FIG. NO.
15 mts.	dendrite -- uniform	43	dendritic-thinner than 304-uniform	35
30 mts.	Coarse dendritic arms	44	arms thickening	36
1 hour	very small equiaxed particles-uniform	46	fragmented dendrites	37
2 hours	Preferential precipitation along grain boundaries	47	fragmented carbide dendrites	38
4 hours	Continuing towards interior	48	together with equiaxed particles	39
6 hours	large equiaxed particles around grain boundaries	49	very coarse dendrites	40
12 hours	with smaller ones farther away	50	equiaxed particles around grain boundaries-smaller in size and less in number.	41

The reasons for the above sequence of precipitating morphology based upon theoretical considerations have been discussed in Chapter IV (Section D).

With progressive increase in the time of sensitisation, these equiaxed particles become more and more localised along the grain boundaries. Figure 50 shows a typical distribution of these carbides for long sensitisation time (12 hours). The large coarse equiaxed carbides may be seen along the grain boundary area, while relatively smaller ones are some distance away from the boundary region. Figure 47 very clearly shows how the localised attack in the sensitised condition starts from the grain boundaries and spreads towards the interior. It is interesting to note that the outline of this corrosion path has a definite geometric pattern.

Thus, it may be concluded that in the initial stages of sensitisation, the carbides are spread throughout the matrix and have a dendritic shape. But, with the increase in the time of sensitisation, these particles become equiaxed. They coarsen and finally align themselves along the grain boundaries.

CHAPTER IV

DISCUSSION

PART A ROLE OF MOLYBDENUM

The application of a proposed theoretical model to explain the improved corrosion-resistance of molybdenum-bearing austenitic stainless steels in sensitised condition.

The improved corrosion resistance of Molybdenum-bearing Austenitic stainless steels has been demonstrated by optical and Electron Microscopy. Most of the works regarding the effect of alloying elements on corrosion behaviour of metals, capable of being passivated in general, and of Austenitic stainless steels in particular, have been directed to correlate the nature of attack with electro-chemical parameters (e.g. Breakdown Potential) and the properties (viz thickness, structure and composition) of the passive film.

A theoretical model is proposed based upon the following considerations:

(1) THERMODYNAMIC ANALYSIS: The relative stability of the various carbides capable of being precipitated in the temperature range under consideration will be examined;

(2) KINETIC ANALYSIS: Taking the planar interface of the grain boundary as a diffusion-front the flux of the various reacting species will be considered;

(3) ELECTRO-CHEMICAL ANALYSIS: As affected by the first two factors.

(1) THERMODYNAMIC ANALYSIS

Consider an austenitic stainless steel with Molybdenum (316 or 316L) in sensitised condition (i.e. heated to 650°C and slowly cooled to room temperature) subjected to corrosive attack in a chloride medium. The localised corrosion which will set forth will be a strong function of the composition and morphology of the carbides precipitated during the sensitisation range of temperature.

The possibility of formation of the various carbides will be governed by the thermodynamic principle of "Free Energy of Formation should be Negative". This aspect is investigated for the various carbides under consideration:

Carbides of Chromium at 650°C

I $1/3\ Cr + C = 1/3\ Cr_3C_3$ $\Delta G^\circ_T = -13,900 - 2.05\ T$

$= -14,790$ Cal at 650°C.

II $23/6\ Cr + C = 1/6\ Cr_{23}C_6$ $\Delta G^\circ_T = -16,380 - 1.54\ T$

$= -17,800$ Cal at 650°C.

Such high negative values of free Energy of formation suggests that both these carbides have thermodynamically a very strong tendency of precipitation.

Carbide of Molybdenum

III $2\ MO + C = MO_2C$ $\Delta G^\circ_T = +4,200 - 4.8\ T$

-120 Cal at 650°C.

This shows that Molybdenum Carbide may not be precipitated

as a separate carbide in the sensitising range of temperature. However, to a very limited extent, Molybdenum may combine with Chromium Carbide to form Complex Carbides of Molybdenum, Chromium and Iron. This would reduce the activity of Chromium in the Carbide, which would indirectly mean that it would lead to greater availability of Chromium in the austenite matrix -- a condition helpful for improved corrosion resistance. But, the kinetic implications of this fact, that Molybdenum Carbide cannot be formed are much more important, which is discussed in the next section.

Effect of Nickel

Nickel distributes itself between austenite and carbide. Philibert et al[37] have shown that the carbide contains only half as much nickel as the average steel content. Nickel will, thus, diffuse away from the growing carbide into the austenite. However, in agreement with Hillert et al[41], this effect is probably of minor importance as compared to the diffusion of chromium to the carbide.

(2) KINETIC ANALYSIS

Consider the transformation of austenite to a layer of carbide. Taking the planar interface of the grain boundary as a diffusion-front, it becomes suggestive from the thermodynamic analysis just considered, that chromium will be diffusing towards the interface, and Molybdenum away from the interface due to the negligible probability of formation of Molybdenum carbides.

In the analysis shown in Appendix I, chromium concentration at the grain-boundary is assumed to be Zero (the validity of which has

been justified in the absence of other substitutional elements).

But, when Mo is present:

(a) Counter-diffusion currents are set in;

(b) Both chromium and Mo have strong attractive forces with carbon ($\epsilon_C^{Mo} = -4.28$ and $\epsilon_C^{Cr} = -5.08$ at 1560°C[64] - data for lower temperatures are not available. But, it is assumed that same behaviour will also be demonstrated at lower temperatures).

Thus, if Molybdenum is to diffuse in a direction opposite to that of Chromium and Carbon, then in order to justify the attractive forces of Molybdenum with Carbon, it has to reduce the flux of carbon towards the grain boundary. This would mean:

(1) that less amount of Carbon will be available to form the carbides at the interface;

(2) and the surplus chromium which cannot combine with carbon to form chromium carbide would be available in the free-form in the matrix. This is illustrated by the schematic profiles. This amounts to the fact that concentration gradient of chromium (Figure 6b) is reduced.

This analysis is helpful in explaining the electro-chemical behaviour of the alloy, which is discussed in the next section.

(3) ELECTRO-CHEMICAL ANALYSIS

The electro-chemistry of any localised corrosion process can be explained in terms of the concept of local anodes and cathodes. If the sensitised stainless steel is subjected to attack in a corrosive medium, say a ferric chloride solution, the carbides precipitated at the grain boundaries act as local cathodes and the adjoining depleted zone acts as the local anode, Figure 2. The intensity of attack will depend upon the chromium gradient existing between the carbides and

the depleted zone. The steeper the gradient, the more positive will be the electro-chemical potential of the local cell, and, thus, more vigorous will be the subsequent attack.

Thus, in light of the above thermodynamic and kinetic analyses, it is not difficult to understand that due to the addition of Molybdenum, since the concentration gradient of chromium is reduced, the potential-difference necessary to activate the local cell is also lowered.

The carbon content of the steel also greatly affects the electro-chemistry of the local cell. Lower the carbon, lower will be the amount of carbide formed. This would imply:

(a) lower cell-voltage and consequently lower rate of attack;

(b) lower cathode to anode area ratio. This essentially means that intensity of attack at local anode points is reduced.

Both these factors demonstrate the improved corrosion resistance of grades containing lower carbon. Thus, "extra-low carbon" grades are specifically used in applications where steel is subjected to attack in highly corrosive media. But, even with "E. L. C. grades", 316L will be more resistant to localised attack than 304L.

Support to this proposed model is given by the Electron Micrographs of the carbide extraction replicas. By comparing Figures 35-41 vs. 43-50, it is seen that the amount of carbides precipitated is lower for 316 as compared to 304 grades. Further evidence to the applicability of this model is provided by the arguments given in Section IV D.

PART B ROLE OF CARBON

The results given in Chapter III show that the intensity of attack is significantly greater for the grades having higher percentage of carbon.

The theoretical basis for this phenomenon is not difficult to understand. Higher the percentage of carbon, greater will be the amount of carbides precipitated; and, thus, the number of available local cells (comprising of carbides as the cathode and the surrounding depleted zone as the anode) will be more. Hence, the total potential generated to give rise to the resulting attack will be more.

Further, commercial grades with higher percentage of carbon are also associated with greater amount of segregated impurities introduced during the course of melting. These impurities act as nuclei to initiate localised attack.

PART C ROLE OF PASSIVE FILMS

A thin protective film (of either an oxide, or of an adsorbed layer of oxygen) is formed on the surface of stainless steel and the local breakdown of this is the cause of pitting. The thin film produced on the surface by the passivation treatment in 2% HNO_3 gives the steel more protective properties to combat localised attack in alcoholic ferric chloride than when the steel is in "active" condition. (A measure of this is the comparison of time to initiate attack as given in Table II.) Further, the passive film produced on the surface of 316 has better protective and "self-healing" properties as compared to that of 304.

It has been claimed by Rhodin[16] that passive films of 316 and 316L consist of ultra thin layer (30 - 60 Å) of oxides of iron, chromium, Molybdenum and amorphous silica. Water is an important constituent of this film, but is not combined in any fixed proportion. This amorphous film has gel-like properties[16,65]. This gel with Mo and

Si has very high viscosity and greatly retards the penetration of the surface by foreign ions like chlorine.

Compositional Data of Passive Films

Compositional data for films of Type 304, 316 and 347 have been determined by Rhodin by X-ray and Calorimetric analysis[16]. The analysis of the film shows that as compared to the parent matrix iron content in the passive film is depleted by 50% and silicon is enriched by a factor of 20. According to his data, passive films of both 304 and 316 showed no enrichment in chromium. In addition, no significant redistribution in nickel was observed. Silicon which was present only as a minor constituent (0.3 to 0.5%) shows maximum enrichment. In Grade 316, there is also an enrichment of Molybdenum by a factor of 2 in the film.

Structural Properties of Passive Film

Study of isolated films by electron diffraction yields diffuse patterns indicative of a finely crystalline nature approaching an amorphous state. Fontana[65] points out that the passive films of thickness 30-50 Å of 304 and 316 are hydrous oxides with water forming up to 30% by weight of the oxide. Transitions in the appearance of the film can be observed as water is adsorbed or desorbed.

(i) It has been pointed out by Rhodin[16], that corrosion resistance of passive film is observed to decrease with increasing film thickness. This may be attributed to the greater chances of breakdown due to accompanying heterogeneity associated with films of greater thickness.

(ii) The composition of the film corresponding to passivity and corrosion resistance is dependent upon the medium in which the film is formed.

PART D EFFECT OF CARBIDE MORPHOLOGY ON THE CORROSION BEHAVIOUR OF AUSTENITIC STAINLESS STEELS IN SENSITISED CONDITION

The complex carbides which are precipitated at the grain boundaries of the Austenitic Stainless Steels during the process of sensitisation are cathodic with respect to the rest of the matrix. Consequently, active local cells are set up, the driving force for which is the potential difference between the carbides (acting as cathodes) and the adjoining depleted zone (anode).

The electro-chemical behaviour is considerably affected by the morphology of the carbides precipitated. Aust et al[42,43,44] have proposed that CONTINUOUS grain boundary precipitates are more deleterious for corrosion resistance than DISCONTINUOUS DESCRETE PARTICLES. This statement is supported by the explanation that in the latter case discontinuities in the corrosion path reduce the probability and intensity of attack. It is felt, that though the above may essentially be applicable for overall corrosion rates, but it may be a misleading index for localised corrosion. For, a factor which profoundly effects localised corrosion behaviour is the active anode to cathode surface area ratio. Lower the value, more intense will be the localised attack even though in certain cases, the overall rate may not be high. Descrete particles may expose greater surface area than continuous carbides (provided the total volume is the same in both the cases).

Hence, in the former case, even though the corrosion rate may be lower (as pointed by Aust et al) yet localised corrosion may be more intense due to the lower anode/cathode surface area ratio. The picture is qualitatively explained in Table IV.

Thus, generalisations about the electro-chemical behaviour cannot be made just on the basis of continuity of discontinuity of the carbide precipitates. A further study has to be made regarding the orientation, stability, size and distribution of these precipitates.

With these theoretical considerations in mind, the carbide precipitates extracted, as given in Chapter III D, will be analysed. On the basis of the electron microscopic studies, the following correlations are attempted:

(a) the effect of sensitisation time on carbide morphology and subsequently on corrosion behaviour;

(b) the effect, if any, of the alloying elements like Molybdenum, upon the carbide distribution. This is attempted by comparing the extracted replicas of AISI 304 and 316 with identical thermal treatments.

(a) The results obtained are in considerable agreement with the theoretical thermodynamic "energy minimum" principle. In the initial stages of precipitation, i.e. around 15 minutes to 30 minutes, the shape of the precipitate is dendritic and these are more or less uniformly distributed throughout the matrix. This denotes a rather unstable configuration due to the increased surface area exposed by the precipitate.

TABLE IV

NATURE OF PRECIPITATE	ANODE TO CATHODE S. A. RATIO	OVERALL CORROSION RATE	INTENSITY OF LOCALISED ATTACK
CONTINUOUS	HIGHER	HIGHER	LOWER
DISCONTINUOUS AND DISCRETE	LOWER	LOWER	HIGHER

But, from the corrosion-resistance standpoint, the dendritic configuration is helpful in so far as the compositional fluctuations between the two dimensional precipitates and the adjoining matrix is not much. Thus, the potential generated between local anodes and cathodes is small. Hence, rate of corrosion is low and there is uniform attack as the carbides are uniformly distributed.

But, with progressive increase in the time of sensitisation, the shape and distribution of the carbide particles undergo a change. The dendritic arms thicken and then fragmentation of these arms take place. With further passage of time, the particles become equiaxed. After 2 hours, for grade 304, coarse equiaxed particles are precipitated along the grain boundaries while smaller ones can be seen in the adjacent areas.

The above observations show that:

(i) in the initial state, due to the dendritic configuration, the overall corrosion rate is lower than that which occurs with roughly equiaxed carbide particles;

(ii) due to the uniform distribution in the early stages, i.e. 15 minutes to 2 hours the attack in corrosion media is not restricted to grain boundary regions, but is uniformly spread throughout the matrix. This is further confirmed by optical photomicrographs (Figures 8, 18, 19); and,

(iii) but, after a critical stage in the sensitisation time, when the particles assume a stable equiaxed or spheroidal configuration and are distributed along the grain boundaries, then preferential attack occurs

along the grain boundaries leaving the interior relatively unaffected.

(b) In the case of AISI 316, the total amount of carbides precipitated is lower due to the presence of Molybdenum (the theoretical basis of which has been explained in Part A of this Chapter). Moreover, the transition from dendritic to equiaxed configuration is delayed as is evident from electron micrographs (compare Figures 47, 48 and 38, 39 for this). This helps in reducing the overall corrosion rates for the Molybdenum-bearing grades. Thus, the presence of Molybdenum has essentially a kinetic, rather than a morphological effect. For, the shape of the precipitates are essentially the same, but the rate of precipitation is altered.

PART E THEORETICAL ANALYSIS OF CORROSION IN ALKALINE MEDIA

The theoretical basis of the attack of austenitic stainless steels in the alkaline medium has to be investigated. When the metal is in the aqueous medium consisting of OH^- ions, as is the case in Kolene, which has 61% sodium hydroxide, the OH^- ions, like the $C\ell^-$ ions, are charged, and are likely to approach the anodic parts of the surface, produced by any of the conditions discussed in Chapter I, under the electrical potential gradient, being schematically shown below.

Having reached the metallic surface, they can go no further and the electrical transfer must consist of the movement of metal cation in the opposite direction. They are unlikely to move right into the liquid -- such movement would not produce the state of lowest free energy (Fe^{++} and OH^- ions in water represent an unstable condition), and further, it would involve the crossing

of an activation energy barrier for the positive ions to pass through the relatively positive hydrogen part of the hydroxyl. Thus, the metallic cation will stay in the negative (oxygen) layer of the hydroxyl, sending on the appropriate number of hydrogen particles into the liquid, which will combine with other hydroxyl ions to give water. This is shown in Figure 52a.

$$H^+ + OH^- = H_2O$$

This further explains why anodic reactions give water rather than hydroxides. A protective film will subsequently form as shown in Figure 52b. CORROSION WILL NOT GET IN UNLESS CHLORINE IONS ARE PRESENT. If chlorine ions are present in sufficient number to outnumber the hydroxyl ions over the whole of the surface, the protective film will not be formed, and there will be general corrosion of the type shown in Figure 33 and schematically shown in Figure 52c. This gives a clue as to why the surface has a rough pitted appearance at times after the treatment in "Kolene" solution. Even if relatively few $C\ell^-$ ions are present, small areas may still be present over which corrosion will occur producing metallic chloride, this will interact with the alkali at a short distance, giving a loose membranous blister, which will prevent the alkali from reaching the metal. The combination of small anodes and large cathodic areas leads to intense localised sttack -- thus, giving the rough surface appearance.

The above mechanism is quite suggestive of the reasons for the rough patchy appearance of some batches of sheets being pickled. Those which are contaminated with aggressive ions like chlorine, suffer the consequence of rough surfaces.

CHAPTER V

CONCLUSIONS AND SUGGESTIONS FOR FUTURE WORK

CONCLUSIONS

(i) Sensitised austenitic stainless steels exhibit localised corrosive attack along the grain boundaries and incoherent twin boundaries as against uniform attack throughout the matrix in the solution-quenched condition.

(ii) Longer the time of sensitisation, more localised and severe is the attack along the grain boundaries.

(iii) Molybdenum, as an alloying element of austenitic stainless steels, reduces the severity of localised attack in the sensitised condition. This is demonstrated by a theoretical model based upon thermodynamic, kinetic and electro-chemical considerations and further confirmed by experimental results.

(iv) Higher the percentage of carbon, greater is the intensity of localised attack.

(v) The corrosion behaviour of austenitic stainless steels is greatly dependent upon the morphology of the carbides precipitated during sensitisation. In the initial stages, the carbides exhibit a dendritic configuration and are spread throughout the matrix. This reduces the severity of attack and does not restrict the attack along the grain

boundaries. But, with increasing time of sensitisation, the carbide particles become equiaxed. These equiaxed particles are finally localised along the grain boundaries. This accounts for the highly localised corrosion during the latter stages of sensitisation.

(vi) The pitted appearance of stainless steel sheets in "Kolene", an industrial reagent used for rescaling the sheets before pickling, is due to the contamination caused by chlorine ions.

SUGGESTIONS FOR FUTURE WORK

The observations reported in this thesis suggest a number of directions in which future studies of localised corrosion of austenitic stainless steels may be undertaken. Some of the interesting aspects are listed below.

(i) The quantitative aspects of the effect of alloying elements like Molybdenum upon localised corrosion behaviour of austenitic stainless steels may be understood by correlating the width of the "depleted zone" with the alloying element percentages. This can be done by micro-probe analysis of the depleted zone combined with electron-microscopic studies.

(ii) The corrosion behaviour of these sensitised steels are greatly dependent upon the orientation and stability of the carbide precipitates. It would be interesting to make a detailed analysis of the structure of carbides precipitated,

by X-ray diffraction and electron-microscopic techniques, under various sensitising conditions and correlating these with subsequent corrosion behaviour.

(iii) A theoretical analysis of the kinetics of grain boundary diffusion involved for the various precipitating carbides under different boundary conditions would be helpful in predicting the corrosion resistant properties of these industrial alloys under various working conditions.

APPENDIX 1

Diffusion Kinetics during Grain-Boundary Precipitation of Chromium Carbides[58]

The differential equations for the concentrations of chromium (C_1) and carbon (C_2) as a function of position and time are:

$$\frac{\partial^2 C_1}{\partial x^2} - \frac{1}{D_1}\frac{\partial C_1}{\partial t} = 0 \text{ and } \frac{\partial^2 C_2}{\partial x^2} - \frac{1}{D_2}\frac{\partial C_2}{\partial t} = 0 \qquad (1)$$

where x is the co-ordinate perpendicular to the grain-boundary which is assumed to be the plane x = 0. D_1 and D_2 are the diffusion coefficients of Cr and C, respectively.

Initial Conditions

$$C_1 = C_1^{\circ} \text{ and } C_2 = C_2^{\circ} \text{ at all x and } t = 0 \qquad (2)$$

Boundary Conditions

$$C_1 = C_1^{\circ} \text{ and } C_2 = C_2^{\circ} \text{ at all t and x} \qquad (3)$$

Let the reaction at the g. b. be represented by the simplified expression

$$4Cr + C \rightarrow Cr_4C \downarrow \qquad (A)$$

Based on the above reaction, one of the boundary conditions is:

$$D_1 \frac{\partial C_1}{\partial x} = 4D_2 \frac{\partial C_2}{\partial x} \text{ all t; } x = 0 \qquad (4)$$

This is based on the assumption that reaction (A) is much faster as compared to the mass transport by diffusion. Assuming, that the reaction is in equilibrium at all times, the second boundary condition is:

$$C_1^4 \cdot C_2 = K \text{ all } t,\ x = 0 \qquad (5)$$

Now, equation (5) leads to a non-linear problem, and, thus, a valid approximation is taken at the boundary:

$$C_1 = 0, \text{ all } t \text{ and } x = 0 \qquad (6)$$

This is valid in the absence of other substitutional elements. If other substitutional elements are present, even then the above relation may hold good provided the interaction parameter between the two substitutional elements tends to zero (e.g. in 316, stainless steel, the presence of Molybdenum does not significantly alter the situation, since the interaction of Mo and Cr is very low[64]).

This means that it is assumed that the carbon content is not too low and that $D_C >> D_{Cr}$.

With the help of the above boundary conditions, the solution of the above set of standard diffusion equations become:

$$\text{Cr:}\quad C_1 = C_1^{\circ} \operatorname{erf} \frac{x}{2\sqrt{D_1 t}} \qquad (7a)$$

and

$$\text{C}:\quad C_2 = C_2 \left\{ 1 - \left(\frac{D_1}{D_2}\right)^{\frac{1}{2}} \frac{C_1^{\circ}}{4C_2^{\circ}} \operatorname{erf}\left[\frac{x}{2\sqrt{D_2 t}}\right] \right\} \qquad (7b)$$

Since $C_2 = 0$ at all times, the approximation is only valid when

$$\left(\frac{D_1}{D_2}\right)^{\frac{1}{2}} \frac{C_1^{\circ}}{4C_2^{\circ}} << 1 \qquad (8)$$

It is found that $D_1 = 2 \times 10^{-13}$ cm^2/sec

and $D_2 = 4 \times 10^{-9}$ cm^2/sec

If the alloy contains 18% Cr, $Cr^{\circ} = 0.346$ moles/100 gms.

Based on this, if approximation (8) is to hold good, then:

$$\%C > .346 \times \frac{12}{4} \times \left(\frac{2 \times 10^{-13}}{4 \times 10^{-9}}\right)^{\frac{1}{2}}$$

i.e. %C should be greater than 0.009%.

This is true since the carbon percentage in Austenitic Stainless Steels is about 0.05% to 0.08% maximum. (In case of extra-low carbon grades, it is 0.025% which also is greater than the above value.) Thus, the approximation made in Equation (6) is a valid one. Based on Equation (7), the width of depleted zone, x is calculated as given below:

$$\frac{C_1}{C_1^\circ} = \text{erf}\ \frac{x}{2\sqrt{D_1 t}} \qquad D_1 = 2 \times 10^{-13}\ \text{cm}^2/\text{sec}$$

$$\frac{C_1}{C_1^\circ} = \frac{\text{Chromium content after sensitisation}}{\text{Initial chromium content}}$$

$$= \frac{12}{18} \text{ (from thermodynamic data)}$$

$$= .66$$

$$\text{erf}\ \frac{x}{2\sqrt{D_1 t}} = .66$$

$$\frac{x}{2\sqrt{D_1 t}} = .68$$

The value of x as a function of time of sensitisation at 650°C is as follows:

t (sec)	x cms
1	$.68 \times 10^{-7}$
10	2.1×10^{-7}
10^2	$.68 \times 10^{-6}$
10^3	2.1×10^{-6}
10^4	$.68 \times 10^{-5}$
10^5	2.1×10^{-5}

APPENDIX II

Validity of the Application of Wagner Analysis for the Calculation of Activity Coefficients of Carbon and Chromium

Assuming the alloy to be a "dilute" solution in which Henrian behaviour is exhibited, the activity coefficient of carbon, γ_C, can be expressed as:

$$\ln \gamma_C = \ln \gamma_C^{\circ} + \left\{ x_C \frac{\partial \ln \gamma_C}{\partial x_C} + x_{Ni} \frac{\partial \ln \gamma_C}{\partial x_{Ni}} + x_{Cr} \frac{\partial \ln \gamma_C}{\partial x_{Cr}} \right\}$$

$\longleftarrow$ 1st order terms $\longrightarrow$

$$+ \left\{ \tfrac{1}{2} x_C^2 \frac{\partial^2 \ln \gamma_C}{\partial x_C^2} + x_C x_{Ni} \frac{\partial^2 \ln \gamma_C}{\partial x_C \, x_{Ni}} + \ldots \right\} + \ldots$$

$\longleftarrow$ 2nd order terms $\longrightarrow$

The higher order terms which occur in second set of brackets can be neglected; they are generally small because the product $x_i x_j$ is small.

Thus $$\ln \gamma_C = \ln \gamma_C^{\circ} + x_C \frac{\partial \ln \gamma_C}{\partial x_C} + x_{Ni} \frac{\partial \ln \gamma_C}{\partial x_{Ni}} + x_{Cr} \frac{\partial \ln \gamma_C}{\partial x_{Cr}} - \text{I}$$

Data for the derivative terms in Equation I is obtained from the literature[56,57].

In a similar manner, the activity coefficient of chromium is also computed. But, unfortunately, the value of derivative terms, $\frac{\partial \ln \gamma_{Cr}}{\partial x_{Cr}}$, $\frac{\partial \ln \gamma_{Cr}}{\partial x_{Ni}}$, and $\frac{\partial \ln \gamma_{Cr}}{\partial x_C}$ are not available. For this purpose it is assumed that $x_C \frac{\partial \ln \gamma_{Cr}}{\partial x_C}$ can be neglected as x_C is small (the validity of which

can be doubted). The other term $\frac{\partial \ln \gamma_{Cr}}{\partial x_{Cr}}$ is obtained from the work of Vermelyea[54].

REFERENCES

1. M. G. Fontana and N. D. Greene, "Corrosion Engineering", McGraw-Hill Book Company, New York (1967).
2. H. H. Uhlig, Trans. Met. Soc. AIME, 140, 442 (1940).
3. R. B. Mears and R. H. Brown, J. Electrochem. Soc., 97, 75 (1950).
4. J. Ellis and F. Laque, Corrosion, 7, 362 (1951).
5. M. Frese, Ind. Eng. Chem., 30, 83 (1938).
6. INCO, "Nickel Topics", 4, 7 (1951).
7. I. L. Rosenfeld and I. S. Danilov, Corros. Sci., 7, 129 (1967).
8. F. P. Robinson, Corrosion Technology, 7, 266 (1960).
9. U. R. Evans, "The Corrosion and Oxidation of Metals", Edward Arnold, London (1960).
10. R. B. Mears and R. H. Brown, Ind. Eng. Chem., 29, 1087 (1937).
11. W. Schwenk, Corros. Sci., 20, 129t (1964).
12. M. B. Ives, Private Communications with W. Schwenk (1968).
13. H. J. Engell and N. D. Stolica, Arch Eisenhuttenwes, 30, 239 (1959).
14. N. D. Tomashov, G. P. Chernova, and O. N. Marcova, Corrosion, 20, 166t (1964).
15. B. E. Wilde and J. S. Armijo, Chem. Abs., 23, 208 (1967).
16. T. N. Rhodin, Corrosion, 12, 3 (1956).
17. M. A. Streicher, J. Electrochem. Soc., 103, 375 (1956).
18. N. D. Greene and M. G. Fontana, Corrosion, 15, 1 (1959).
19. T. P. Hoar, Trans. Faraday. Soc., 45, 683 (1949).
20. A. K. Vijh, Corros. Sci., 11, 3 (1971).
21. H. Taube, Chem. Rev., 50, 69 (1952).

22. Ja. M. Kolotyrkin, Corrosion, 19, 8 (1963).

23. O. Steensland, Uddeholm, Report No. 75, (Jan. 1967).

24. V. Hospadaruk and J. V. Petrocelli, J. Electrochem. Soc., 113, 878 (1966).

25. H. H. Uhlig, "Corrosion Handbook", John Wiley and Sons, Inc., New York (1960).

26. I. L. Rosenfeld and I. S. Danilov, Z. Phys. Chem., 226, 257 (1964).

27. E. Brauns and W. Schwenk, Arch. Eisenhuttenwes, 30, 239 (1959).

28. U. R. Evans and R. B. Mears, Proc. Roy. Soc., 146A, 153 (1934).

29. R. Donker and G. Dengg, Korrosion, 3, 241 (1927).

30. E. M. Mahla and N. A. Nielsen, Trans. Electrochem. Soc., 89, 167 (1946).

31. R. Parsons and C. Cudd, J. Phys. Chem., 45, 1339 (1941).

32. C. May, J. Inst. Met., 32, 65 (1953).

33. P. M. Aziz, J. Electrochem. Soc., 101, 120 (1954).

34. B. E. Hopkinson and K. G. Caroll, Nature, 184, 1479 (1959).

35. C. W. Weaver, J. Inst. Met., 90, 404 (1961/62).

36. J. Plateau, Coll. de. Met., Corrosion, 185 (1960).

37. J. Philibert et al, C. R. Acad. Sci. Paris, 251, 1289 (1960).

38. G. Pomey, Trans. Met. Soc. AIME, 218, 310 (1960).

39. M. J. Fleetwood, J. Inst. Met., 90, 429 (1961/62).

40. S. Alm and R. Kiesling, J. Inst. Met., 91, 190 (1962/63).

41. C. O. Stawstrom and M. Hillert, JISI, 207, 77 (1969).

42. J. S. Armijo, K. T. Aust, and J. H. Westbrook, ASM Trans. Quart., 59, 544 (1966).

43. J. S. Armijo, K. T. Aust, and J. H. Westbrook, ASM Trans. Quart., 60, 360 (1967).

44. J. S. Armijo, K. T. Aust, and J. H. Westbrook, ASM Trans. Quart., 61, 270 (1968).

45. H. H. Uhlig, Trans. Electrochem. Soc., 85, 307 (1944).

46. M. Faraday, "Experimental Researches in Electricity", Vol. II, p. 243, Dover (1844).

47. S. Glasstone, "Textbook of Physical Chemistry", p. 1011, S. Van Nostrand Co. Inc., London (1940).

48. R. B. Mears, Trans. Electrochem. Soc., 77, 288 (1940).

49. S. Tammann, Z. Anorg. Chem., 107, 236 (1919).

50. T. P. Hoar, R. B. Mears, G. P. Rothwell, Corros. Sci., 5, 279 (1965).

51. Andreeva, Corrosion, 20, 35t (1964).

52. T. P. Hoar and U. R. Evans, J. Electrochem. Soc., 99, 212 (1952).

53. N. A. Nielsen, Corrosion, 20, 104t (1964).

54. C. S. Tedman, D. A. Vermalyea, and J. H. Rosalowski, J. Electrochem. Soc., 118, 2 (1971).

55. F. D. Richardson, JISI, 167, 33 (1953).

56. B. Floren and J. Hayden, ASM Trans. Quart., 61, 489 (1968).

57. R. Heakler and T. Winchell, Trans. Met. Soc., AIMI, 227, 732 (1963).

58. W. Jost, "Diffusion", Academic Press, New York (1960).

59. P. J. Gellings and M. A. De Jough, Corros. Sci., 7, 413 (1967).

60. J. Shirley and R. Truman, JISI, 171, 354 (1952).

61. W. D. France and N. D. Greene, Corros. Sci., 8, 9 (1968).

62. M. A. Streicher, Corros. Sci., 9, 53 (1969).

63. U. R. Evans, "Corrosion and Oxidation of Metals", First Supplement Volume, p. 359, Edward Arnold, London (1961).

64. Stahleisen, Sonderberichte, Heft, 7 (1968).

65. M. G. Fontana, Corrosion, 3, 567 (1967).

66. D. C. Grahme and R. B. Whitney, J. Am. Chem. Soc., 64, 1548 (1942).

FIGURE CAPTIONS

Figure 1 Typical Anodic Dissolution Behaviour of an Active-Passive Metal.

Figure 2 Schematic Representation of Intergranular Corrosion Caused by the Precipitation of Chromium Carbide.

Figure 3 Schematic Model of a Pit (a) Open Pit; (b) Closed Pit.

Figure 4 Autocatalytic Process occurring in a Corrosion Pit.

Figure 5 Schematic Representation of an Electrical Double Layer formed during Localised Corrosion.

Figure 6a Concentration Profiles during Precipitation of Grain-Boundary Carbides; b, Concentration Profiles of C, Cr, Mo -- Proposed Model.

(Figures 7-51 are optical and electron microphotographs of corrosion studies)

Figure 7 316L -- 1300°C -- ½ hour, WQ, Alcoholic Ferric Chloride, (AFC) 4 hours (120 x).

Figure 8 316L -- 1300°C -- ½ hour, WQ, 650°C -- 2 hours, Furnace Cool, AFC -- 4 hours (120 x).

Figure 9(a) 316L -- 1300°C -- ½ hour, WQ, 650°C -- 4 hours, FC, AFC -- 4 hours (400 x).

Figure 9(b) Same as 9(a) in Passive Condition.

Figure 10 316L -- 1300°C -- ½ hour, WQ, 650°C -- 24 hours, FC, AFC -- 4 hours, S. E. M. (120 x).

Figure 11 316L -- 1300°C -- ½ hour, WQ, 650°C -- 48 hours, FC, AFC -- 4 hours, S. E. M. (240 x).

Figure 12 316L -- 1300°C -- ½ hour, WQ, 650°C -- 48 hours, FC, AFC -- 4 hours, S. E. M. (240 x).

Figure 13 316L -- 1300°C -- ½ hour, WQ, 650°C -- 96 hours, FC, AFC -- 4 hours, S. E. M. (240 x).

Figure 14 Scanning Electron Micrograph of Plastic Replica, Sensitisation time = 48 hours (120 x).

Figure 15 S. E. M. of Plastic Replica, Sensitisation time = 96 hours (240 x).

Figure 16 316L -- Thermal conditions same as in Figure 7, Passivated (120 x).

Figure 17(a) 316 -- 1300°C -- ½ hour, WQ, AFC -- 4 hours (Active) 240 x.

Figure 17(b) same as in 17(a), Passive 240 x.

Figure 18 316 -- 1300°C -- ½ hour, WQ, 650°C -- 1 hour, FC, AFC -- 4 hours (400 x).

Figure 19 316 -- 1300°C -- ½ hour, WQ, 650°C -- 2 hours, FC, AFC -- 4 hours (240 x).

Figure 20 316 -- 1300°C -- ½ hour, WQ, 650°C -- 24 hours, FC, AFC -- 4 hours (400 x).

Figure 21 316 -- 1300°C -- ½ hour, WQ, 650°C -- 48 hours, FC, AFC -- 4 hours (240 x).

Figure 22 316 -- 1300°C -- ½ hour, WQ, 650°C -- 96 hours, FC, AFC -- 4 hours (240 x).

Figure 23 316 -- Thermal treatments same as in Figure 19, Passive (240 x).

Figure 24 304L -- 1300°C -- ½ hour, WQ, 650°C -- 24 hours, FC, AFC -- 4 hours (240 x).

Figure 25 304(1) -- 0.06% C, 1300°C -- ½ hour, WQ, 650°C -- 2 hours, FC, AFC -- 4 hours (240 x).

Figure 26 304(1) -- 1300°C -- ½ hour, WQ, 650°C -- 6 hours, FC, AFC -- 4 hours (400 x).

Figure 27 304(1) -- 1300°C -- ½ hour, WQ, 650°C -- 12 hours, FC, AFC -- 4 hours (400 x).

Figure 28 304(1) -- 1300°C -- ½ hour, WQ, 650°C -- 24 hours, FC, AFC -- 4 hours (400 x).

Figure 29 304(11) -- 0.07% C, 1300°C -- ½ hour, WQ, 650°C -- 24 hours, FC, AFC -- 4 hours (400 x).

Figure 30 304(1), 1300°C -- ½ hour, WQ, 650°C -- 48 hours, FC, AFC -- 4 hours (400 x).

Figure 31 304 (11) -- 1300°C -- ½ hour, WQ, 650°C -- 48 hours, FC, AFC -- 4 hours (400 x).

Figure 32 316L -- 1300°C -- ½ hour, WQ, "Kolene" -- 480°C -- 15 minutes, 240 x.

Figure 33 316L -- 1300°C -- ½ hour, WQ, "Kolene" -- 480 -- 45 min., 240 x.

Figure 34 316L -- Measurement of Pit depth by Interferometry Pit depth = 4 micron.

Figure 35 316 -- Time of sensitisation -- 15 minutes -- two stage Carbide extraction replica (24000 x).

Figure 36 316 -- Time of sensitisation -- 30 minutes (24000 x).

Figure 37 316 -- Time of sensitisation -- 1 hour (24000 x).

Figure 38 316 -- Time of sensitisation -- 2 hours (24000 x).

Figure 39 316 -- Time of sensitisation -- 4 hours (24000 x).

Figure 40 316 -- Time of sensitisation -- 6 hours (24000 x).

Figure 41 316 -- Time of sensitisation -- 12 hours (22000 x)

Figure 42(a) 316L -- Time of sensitisation -- 12 hours (22000 x).

Figure 42(b) 316L -- Time of sensitisation -- 24 hours (22000 x).

Figure 43 304(1) -- Time of sensitisation -- 15 min. (24000 x).

Figure 44 304(1) -- Time of sensitisation -- 30 min. (24000 x).

Figure 45 304(1) -- Time of sensitisation -- 45 min. (24000 x).

Figure 46 304(1) -- Time of sensitisation -- 1 hour (24000 x).

Figure 47 304(1) -- Time of sensitisation -- 2 hours (24000 x).

Figure 48 304(1) -- Time of sensitisation -- 4 hours (24000 x).

Figure 49 304(1) -- Time of sensitisation -- 6 hours (17000 x).

Figure 50 304(1) -- Time of sensitisation -- 12 hours (17000 x).

Figure 51 304(11) -- Enlarged Pit View (65000 x)
Time of sensitisation -- 48 hours.

Figure 52 Schematic representation of corrosion in alkaline media due to contamination with chlorine ions.

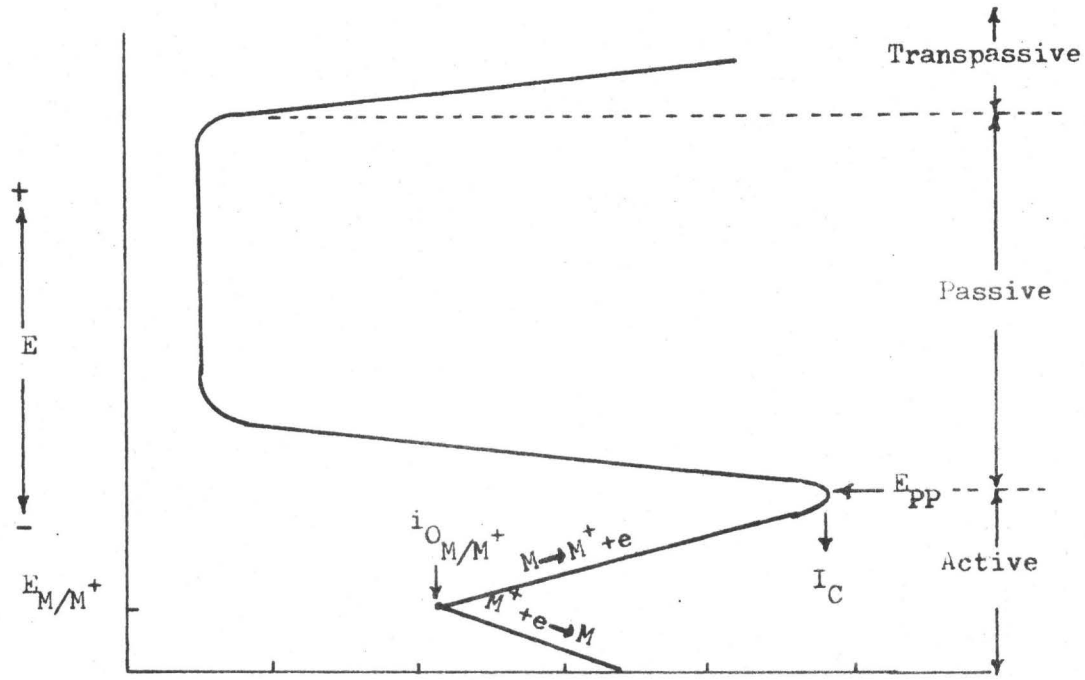

Figure 1

Typical anodic dissolution behaviour of an active-passive metal.

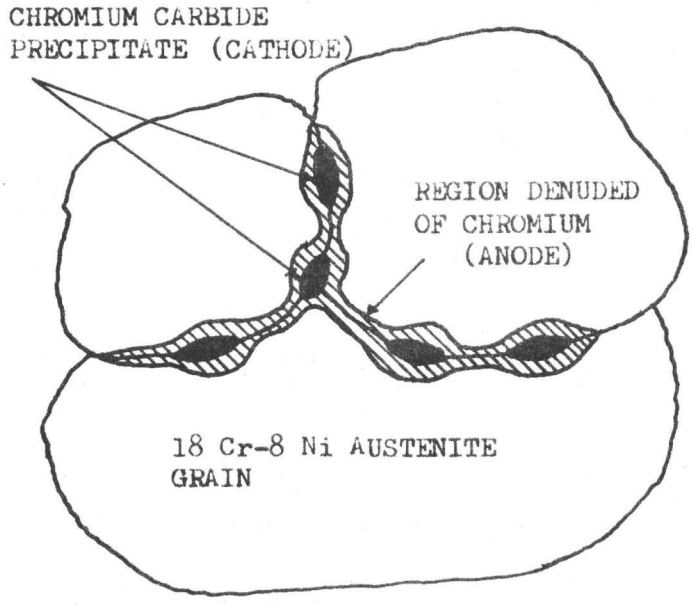

Figure 2

Schematic representation of Active Local Cells in Austenitic Stainless Steel in Sensitised Condition.

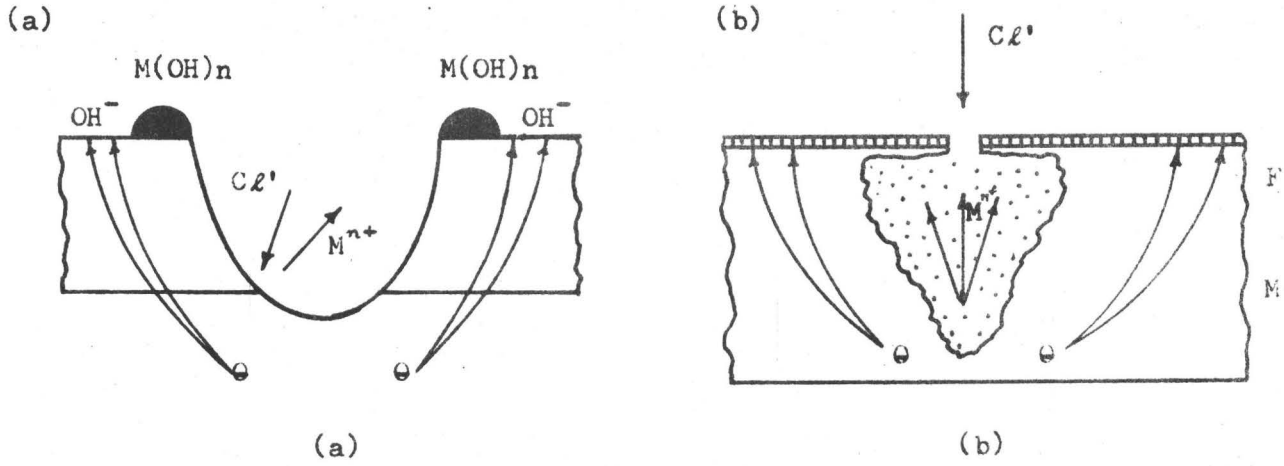

Figure 3

Schematic representation of a pit: a, open pit; b, closed pit.

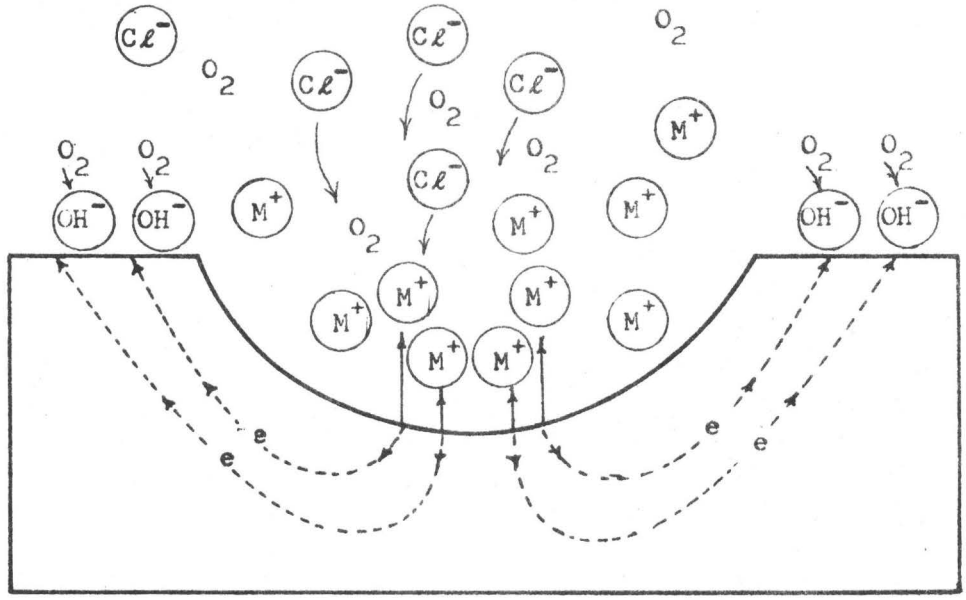

Figure 4

Autocatalytic processes occurring in a corrosion pit.

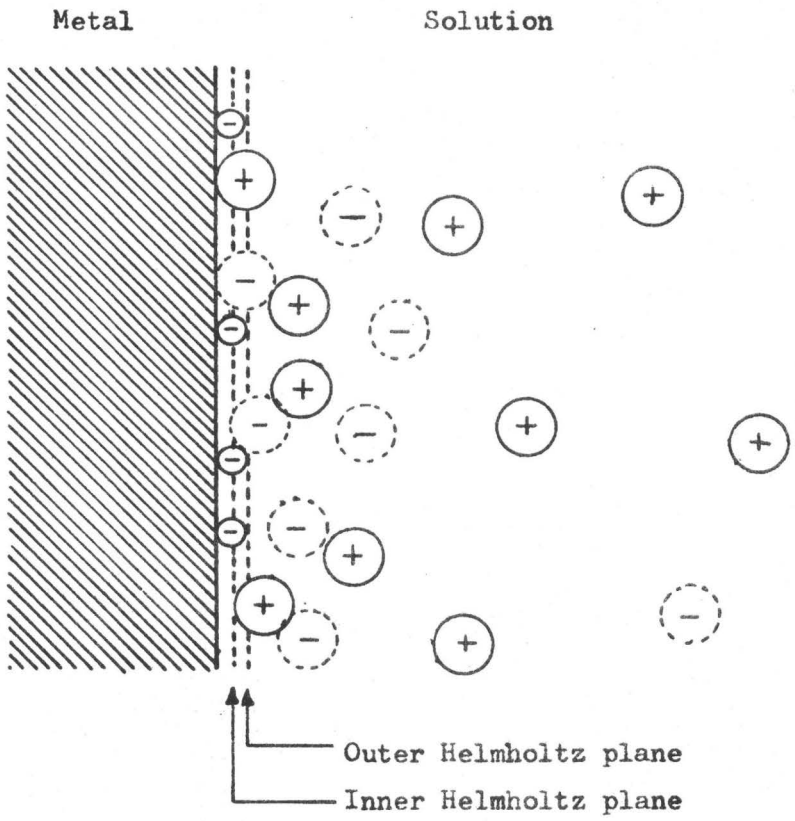

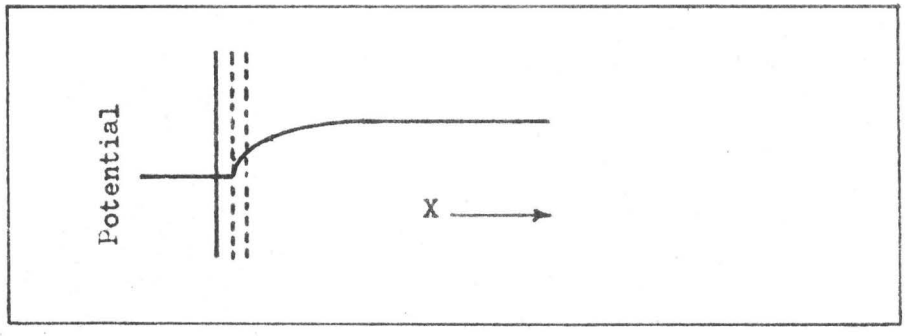

Figure 5
Schematic representation of the electrical double layer when a metal comes in contact with an aqueous solution.

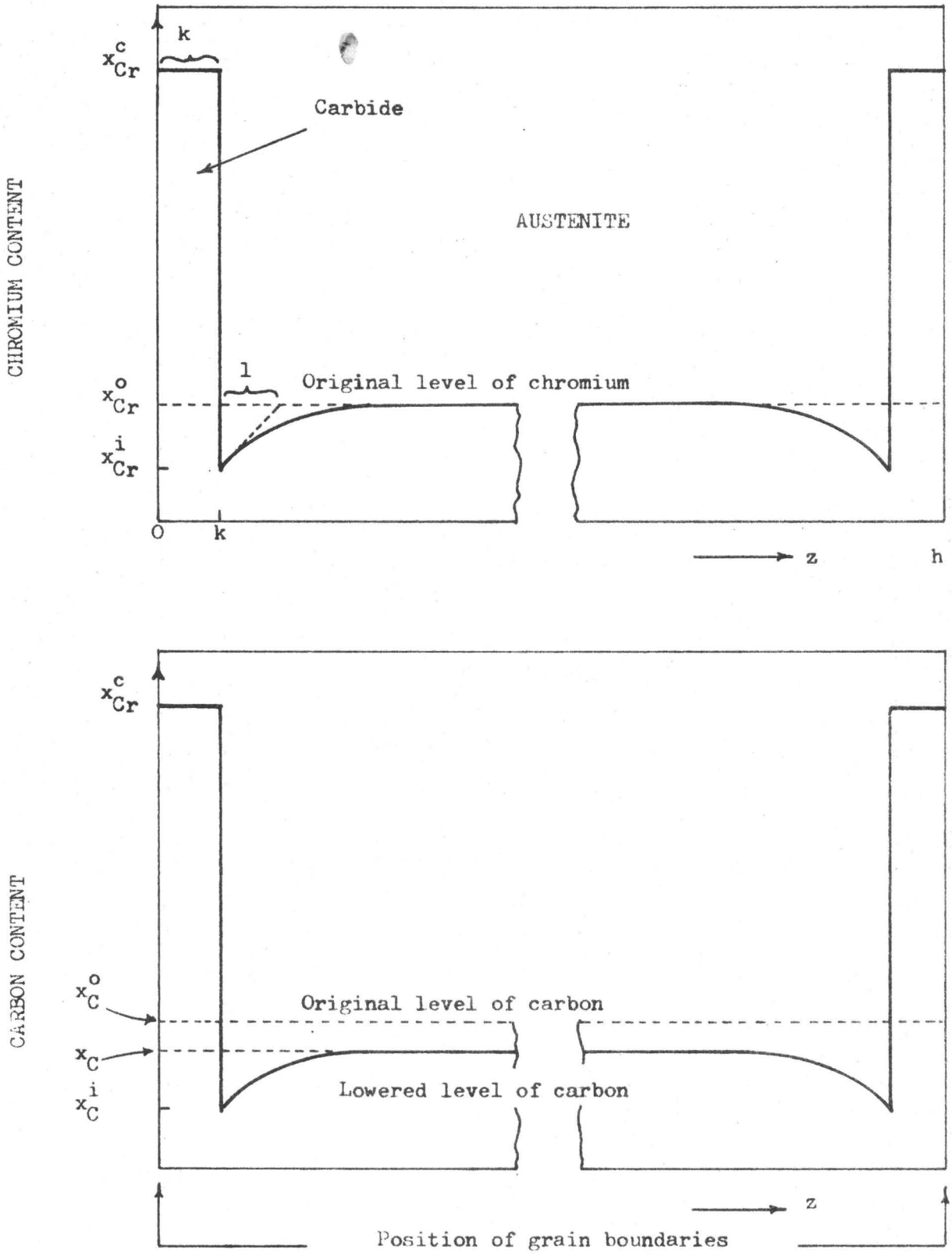

Figure 6(a) Hillert's Model
Concentration profiles during precipitation of grain boundary carbide.

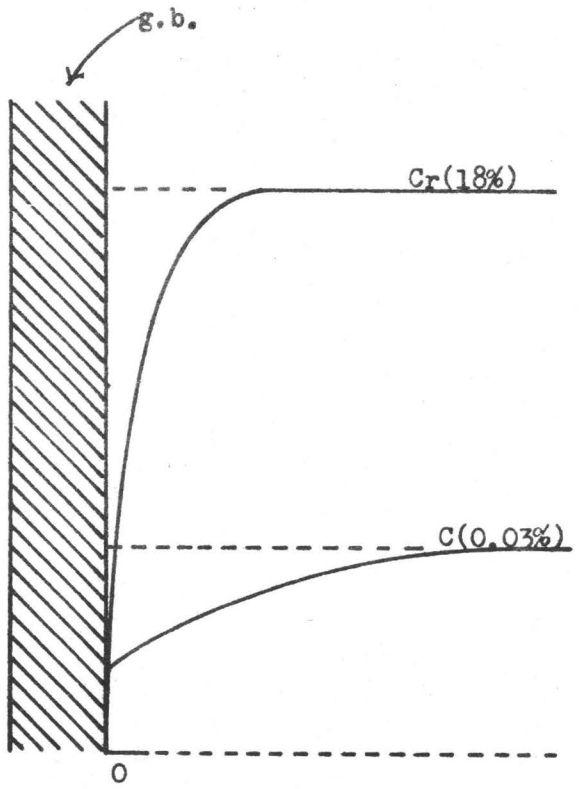

(A) When no Mo present

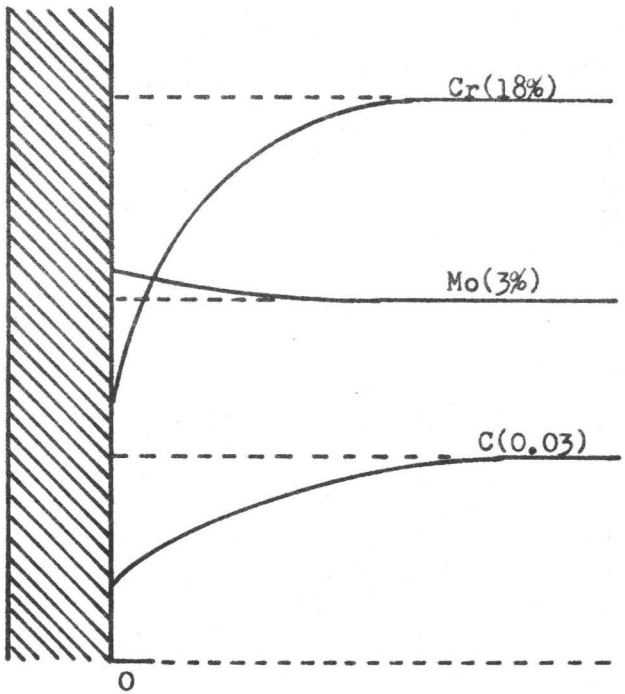

(B) When Mo present

Figure 6(b) Concentration Profiles of C, Cr, Mo -- Proposed Model

Figure 7

Figure 8

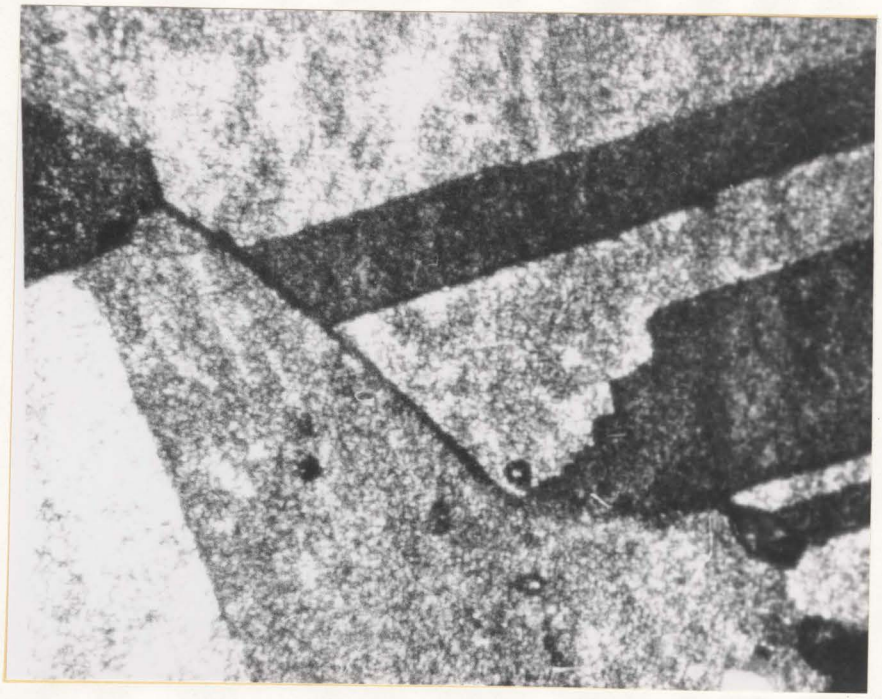

Figure 9a

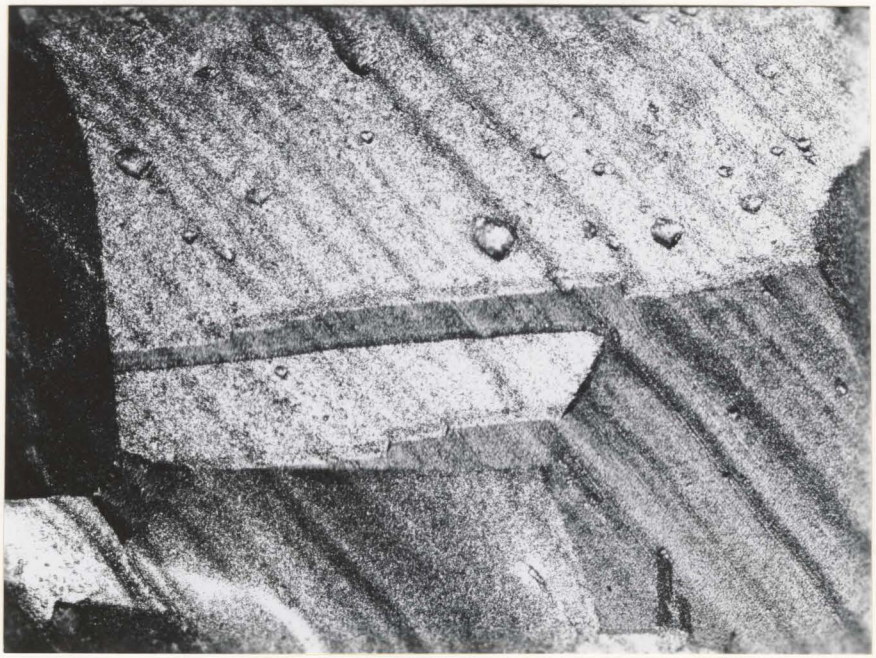

Figure 9b

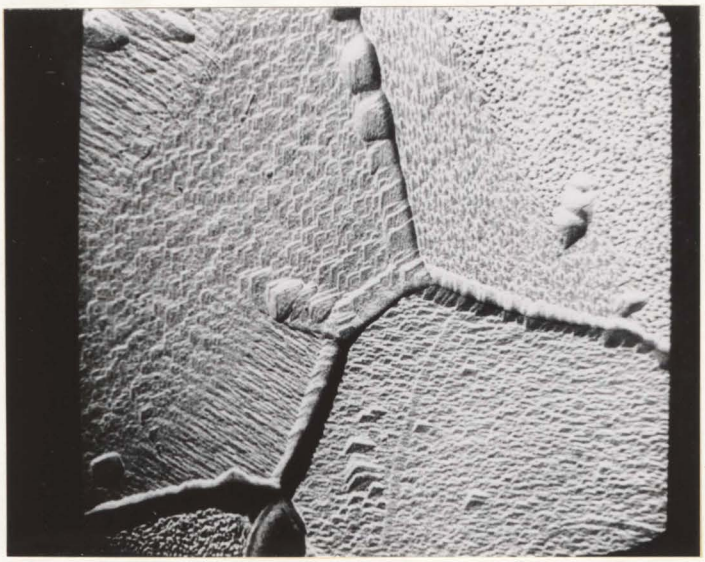

Figure 10

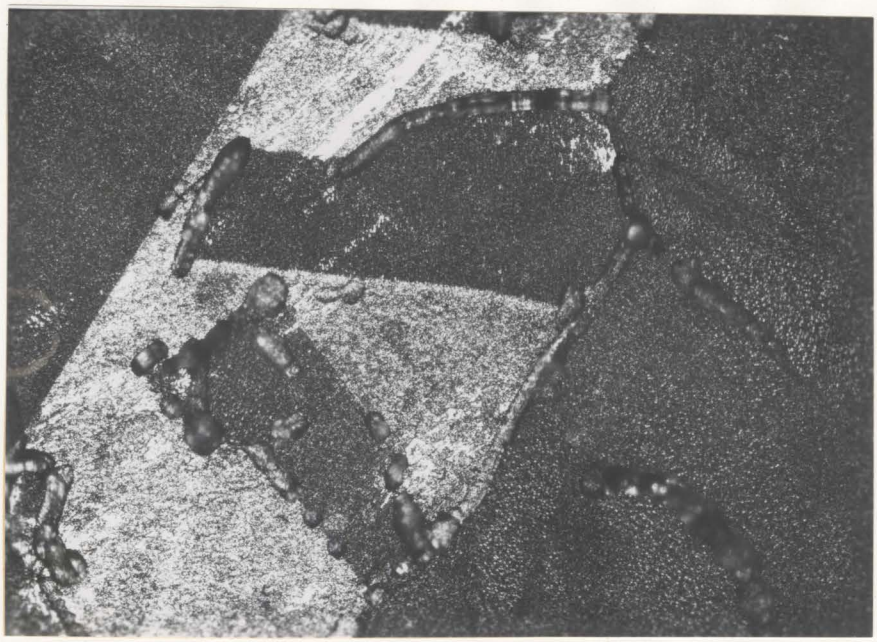

Figure 11

Figure 12

Figure 13

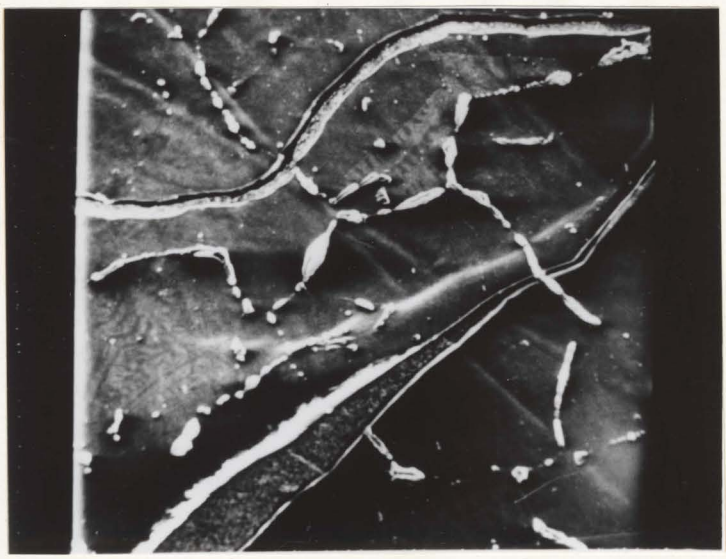

Figure 14

Figure 15

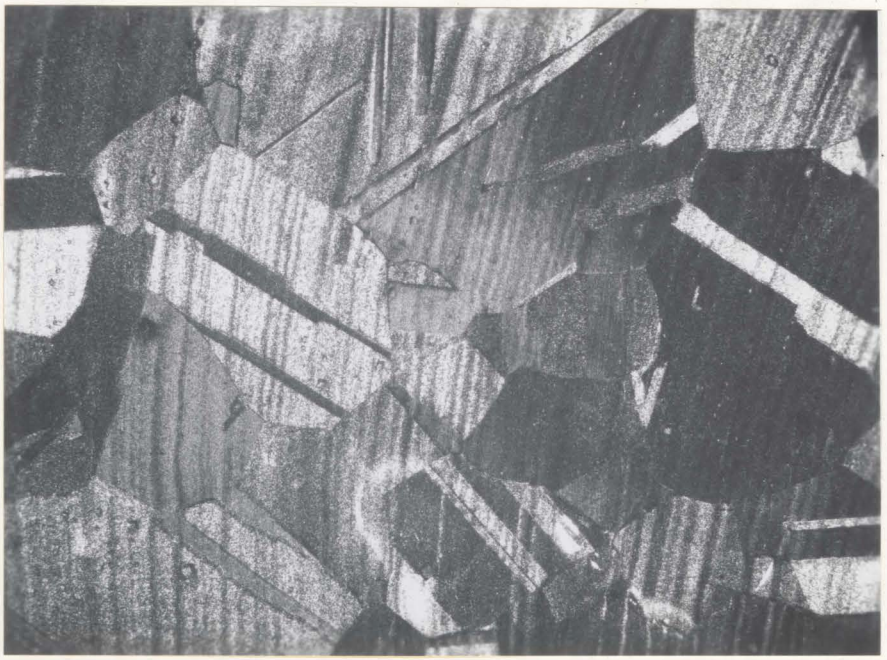

Figure 16

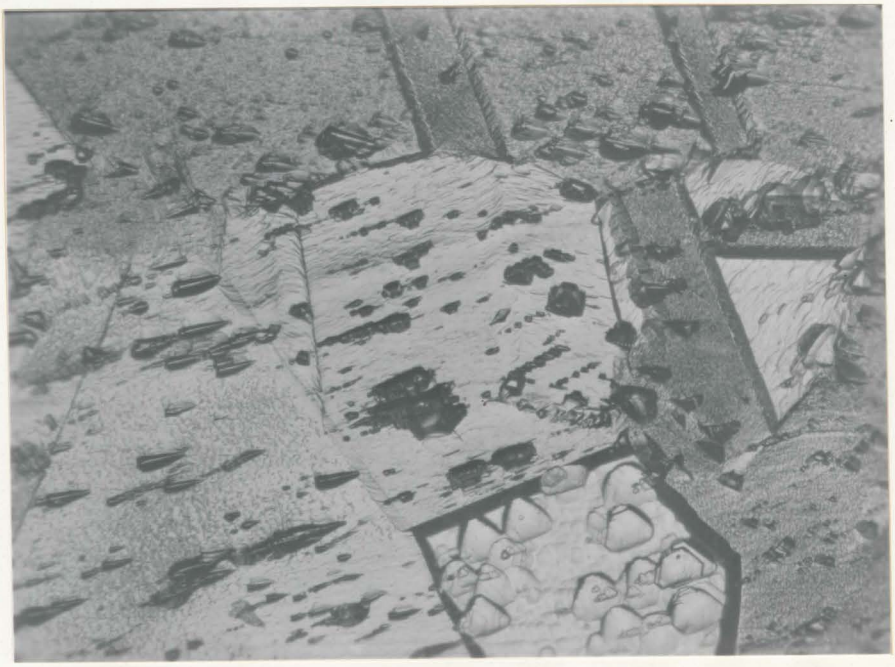

Figure 17a

Figure 17b

Figure 18

Figure 19

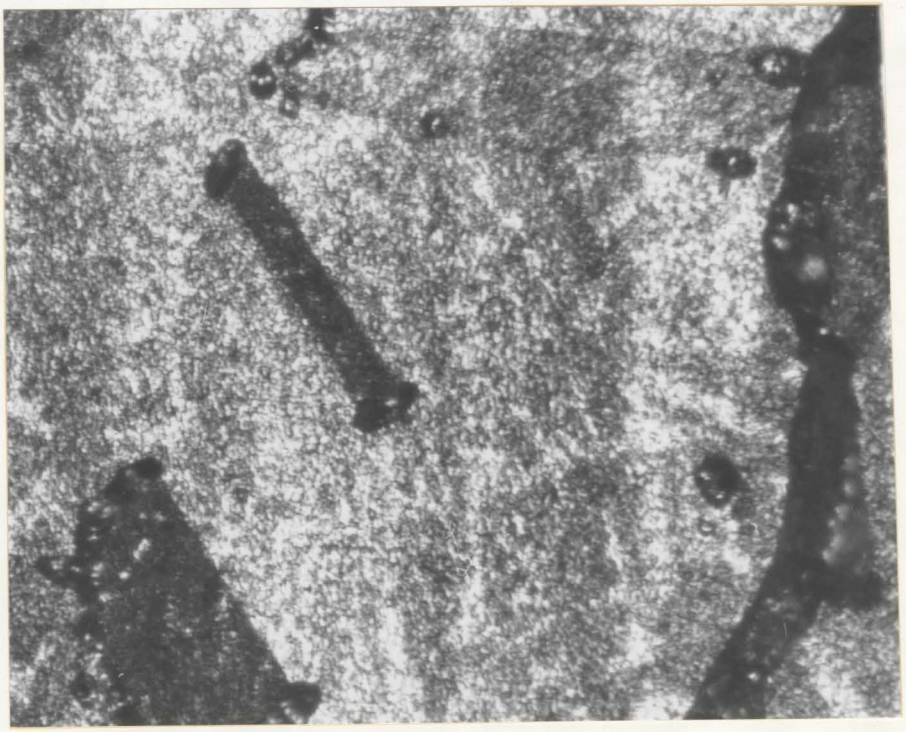

Figure 20

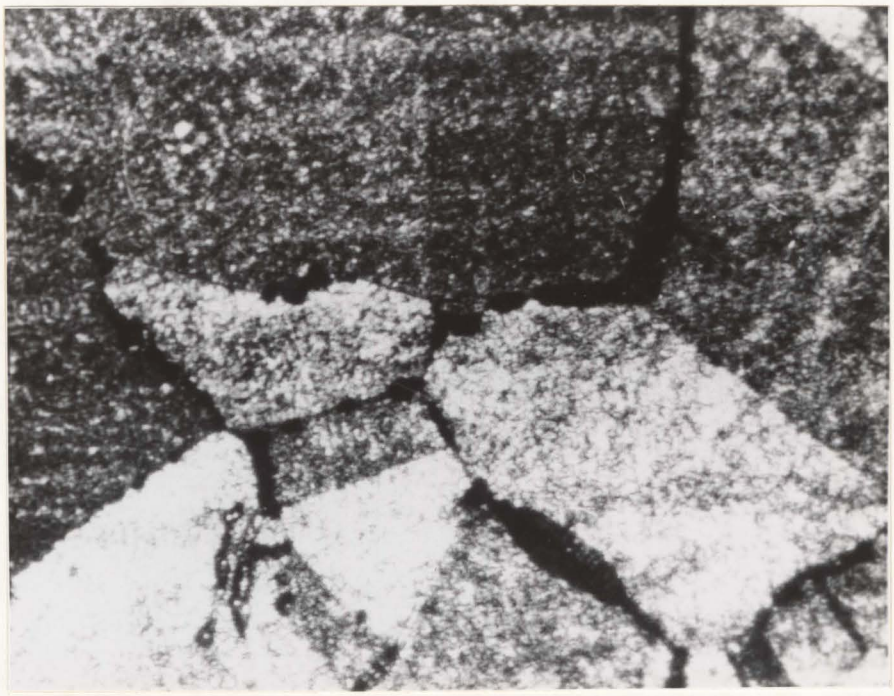

Figure 21

Figure 22

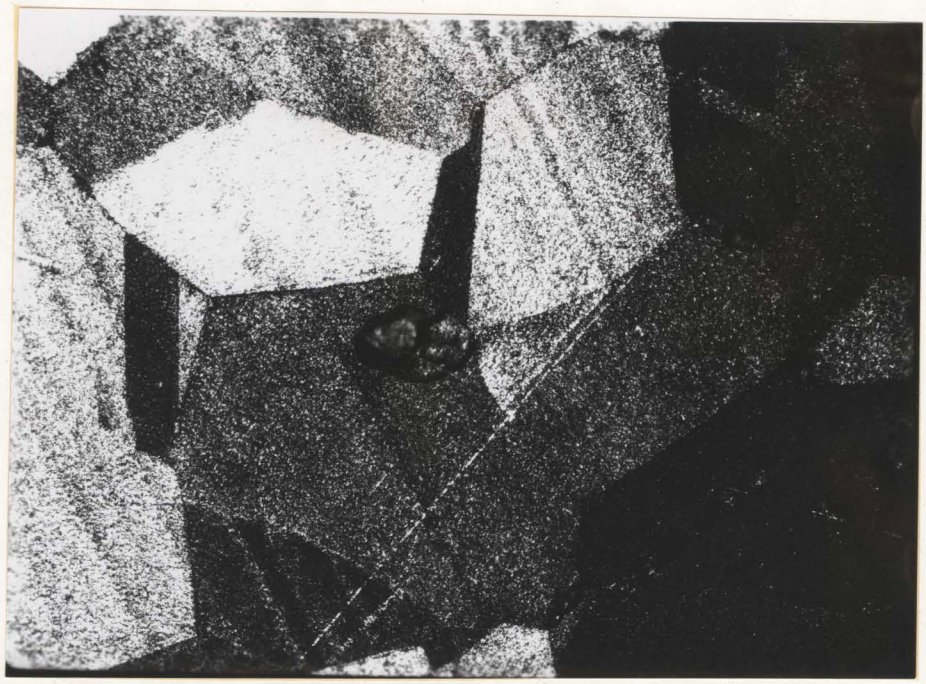

Figure 23

Figure 24

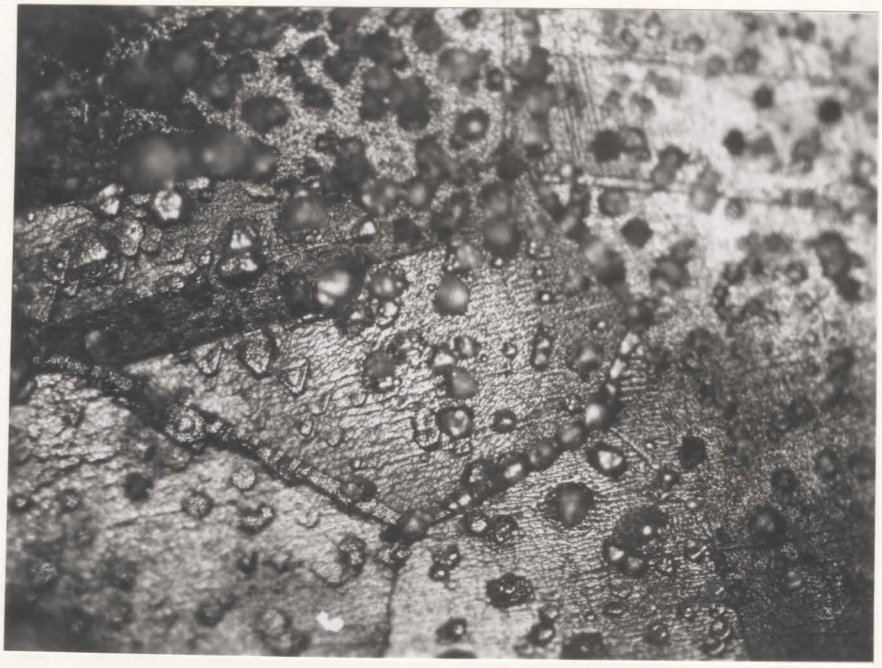

Figure 25

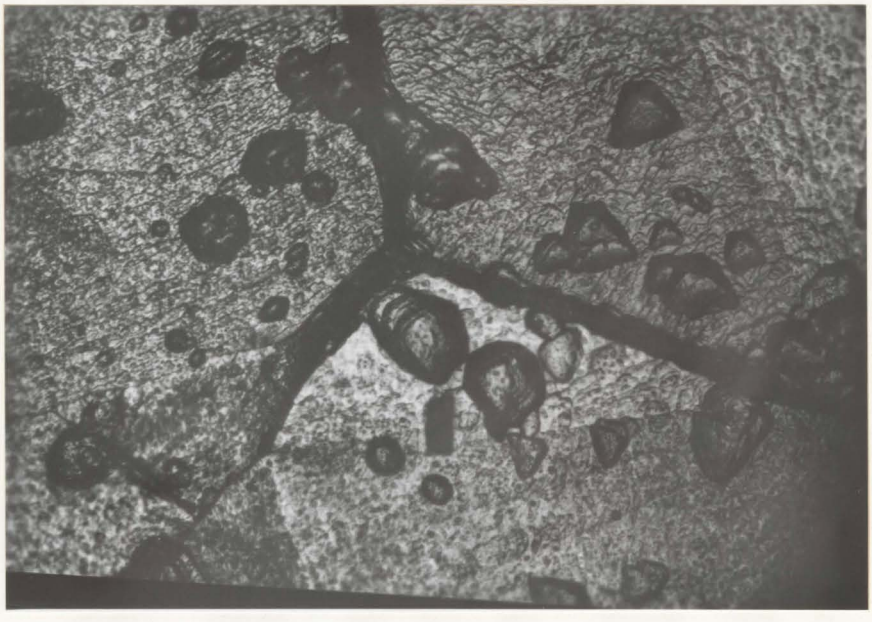

Figure 26

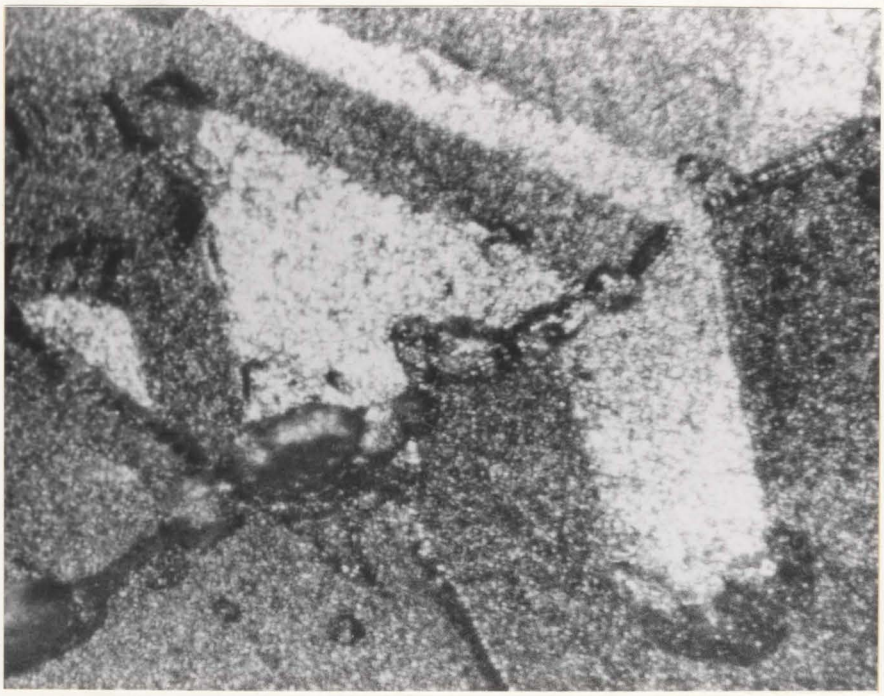

Figure 27

Figure 28

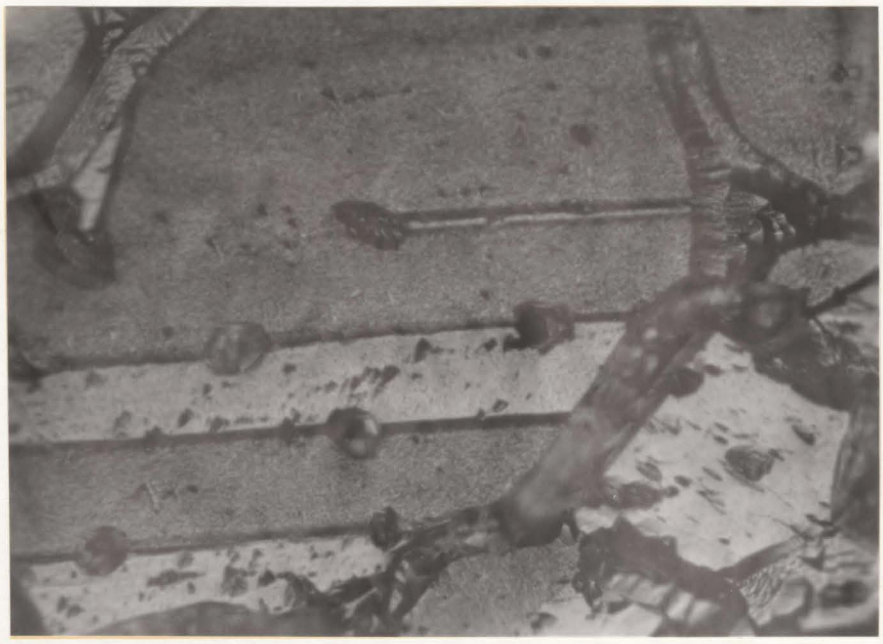

Figure 29

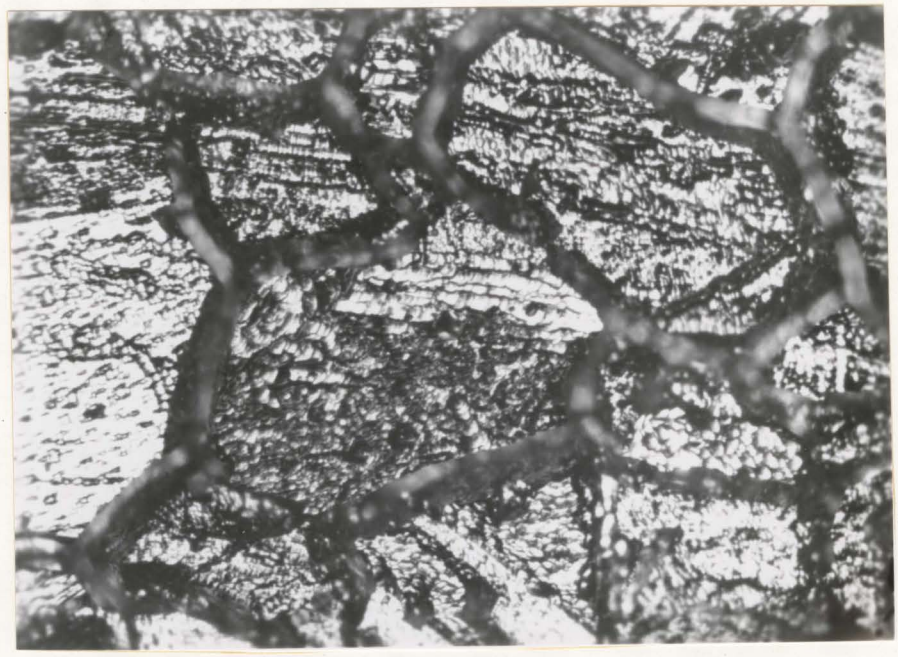

Figure 30

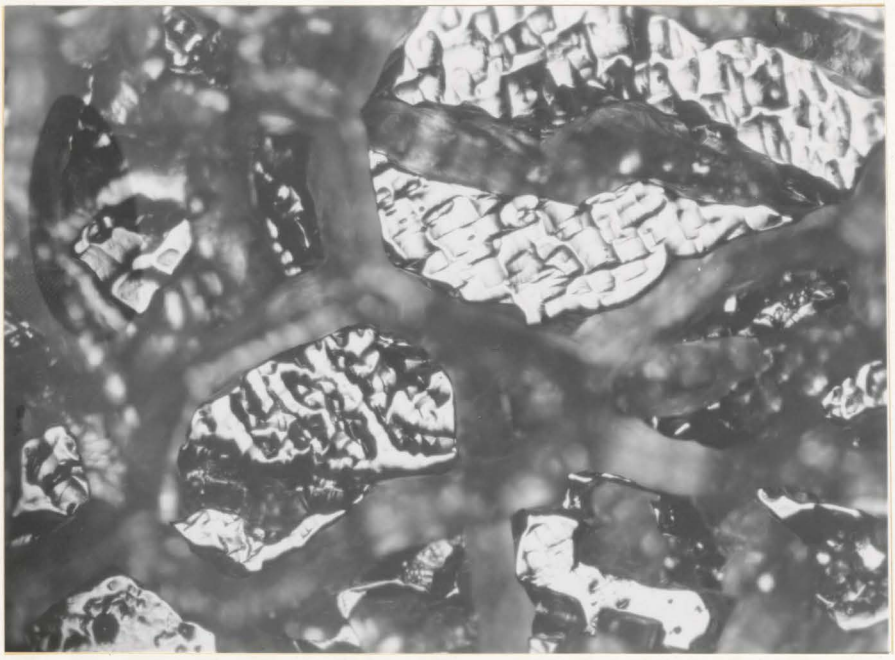

Figure 31

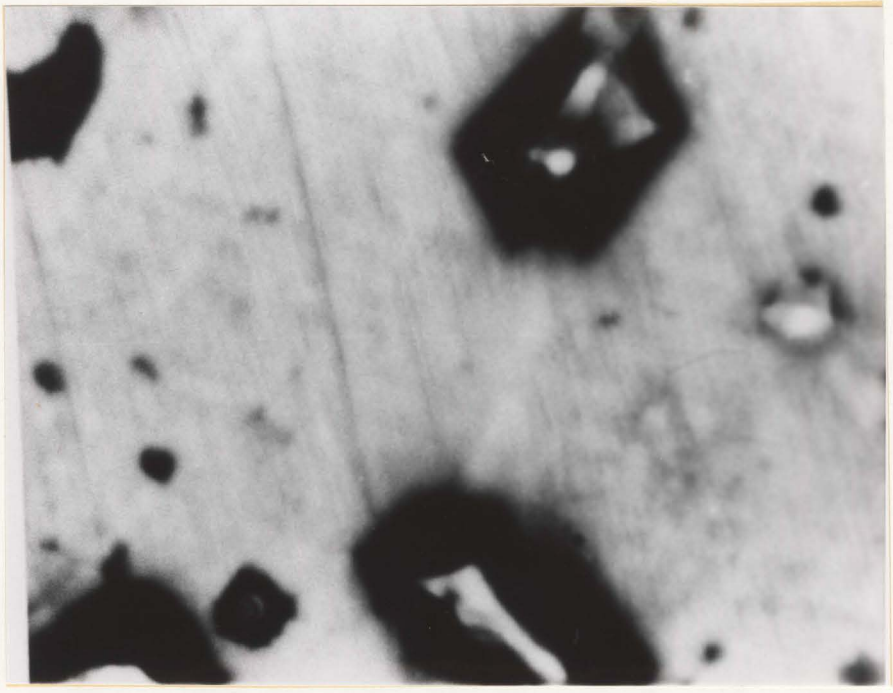

Figure 32

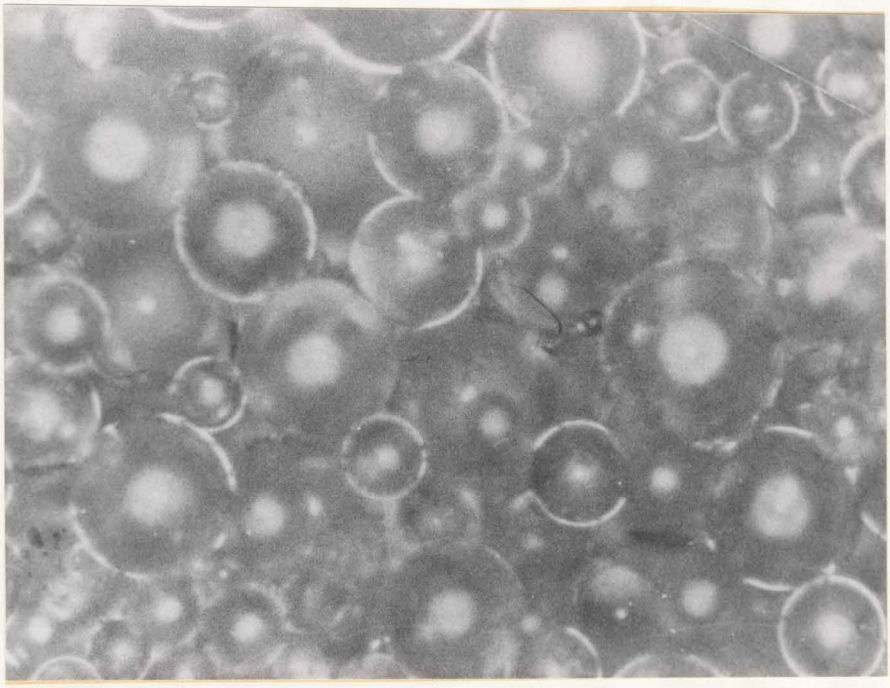

Figure 33

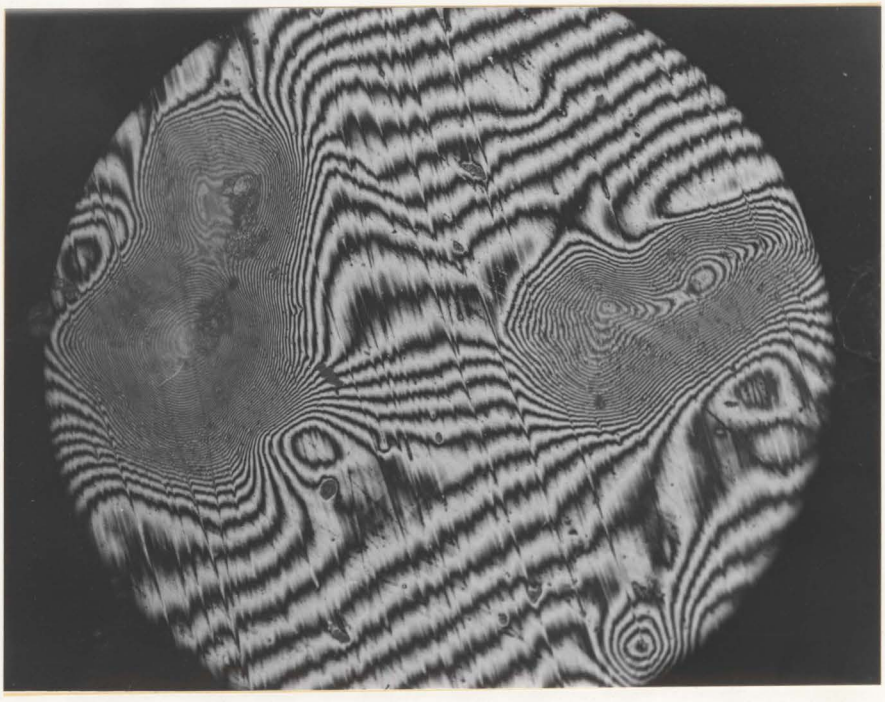

Figure 34

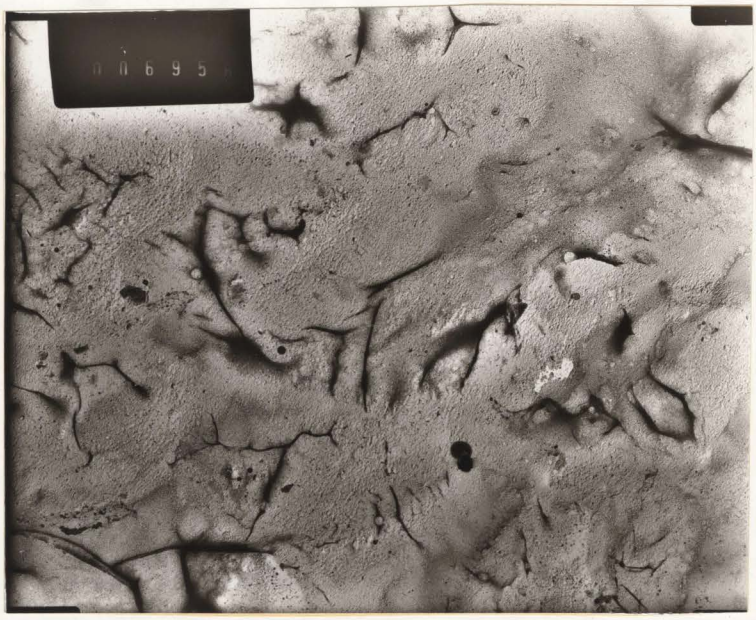

Figure 35

Figure 36

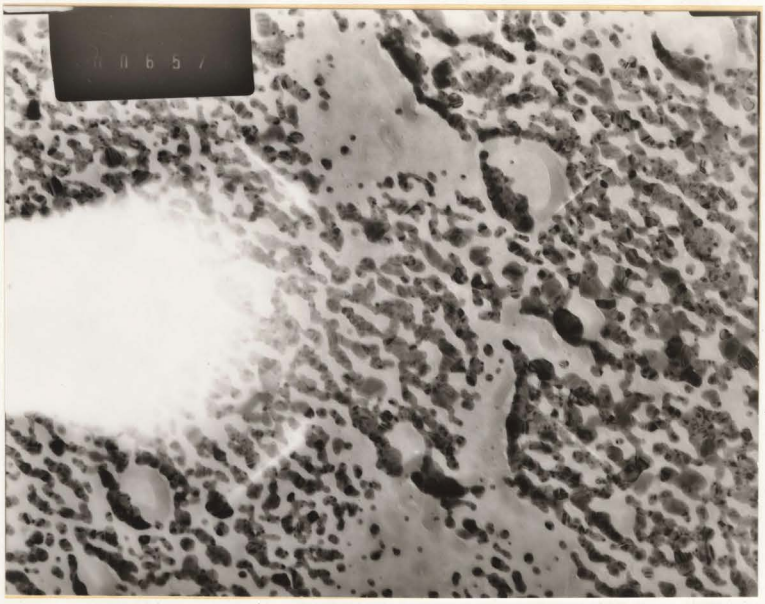

Figure 37

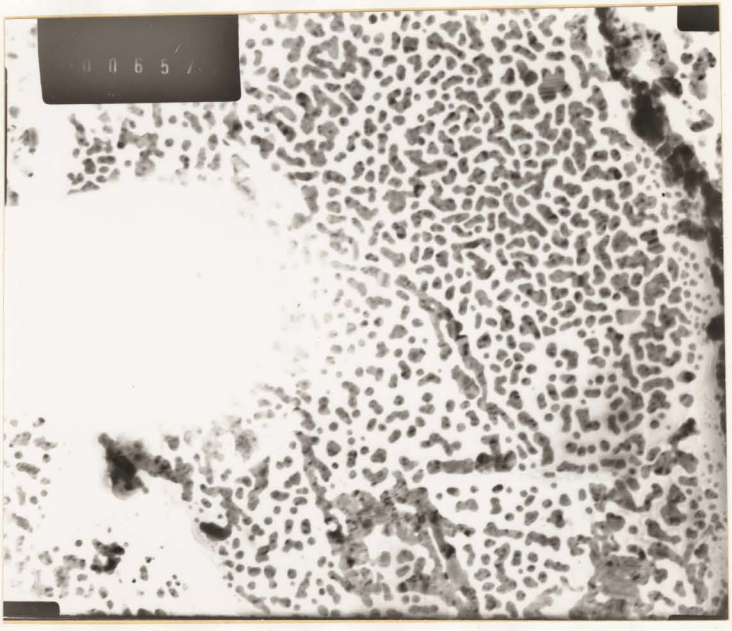

Figure 38

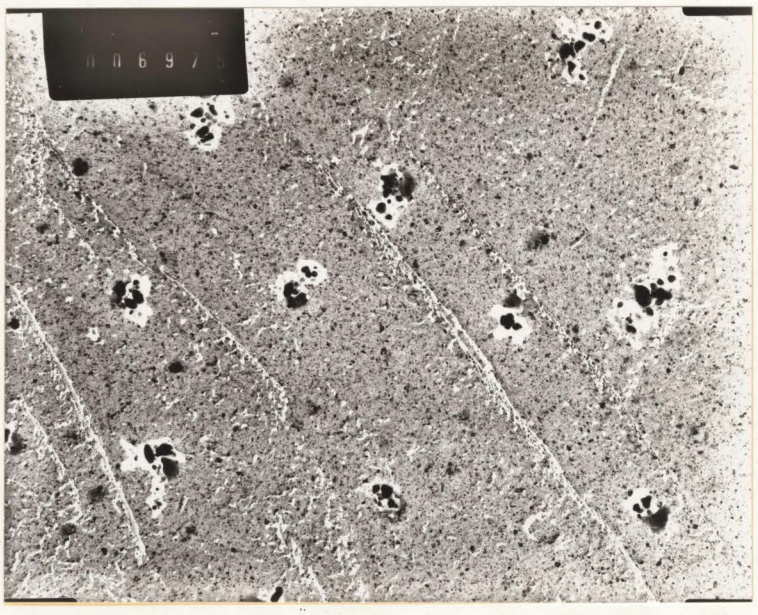

Figure 39

Figure 40

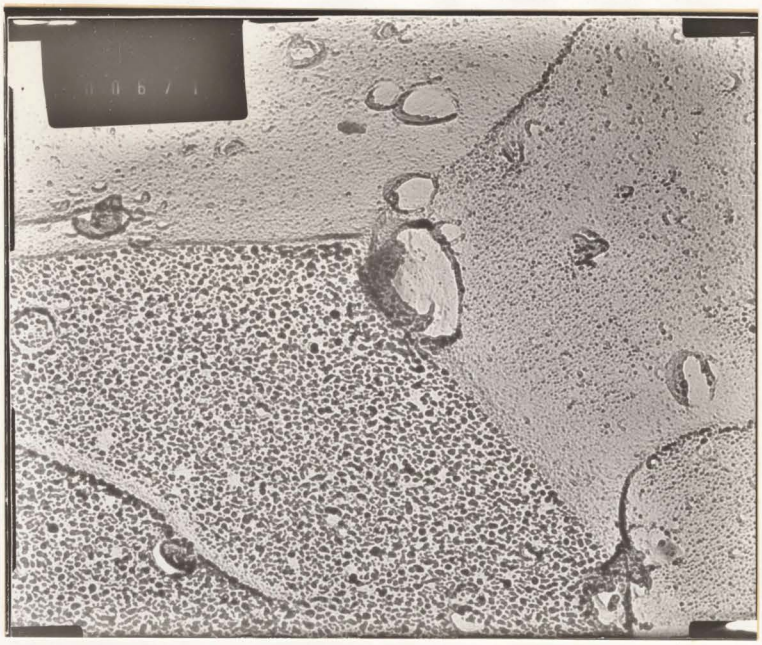

Figure 41

Figure 42a

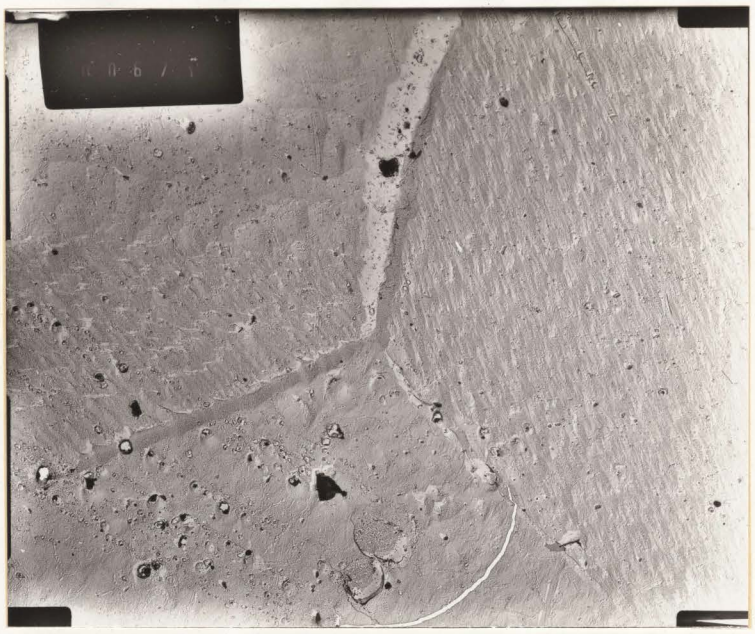

Figure 42b

Figure 43

Figure 44

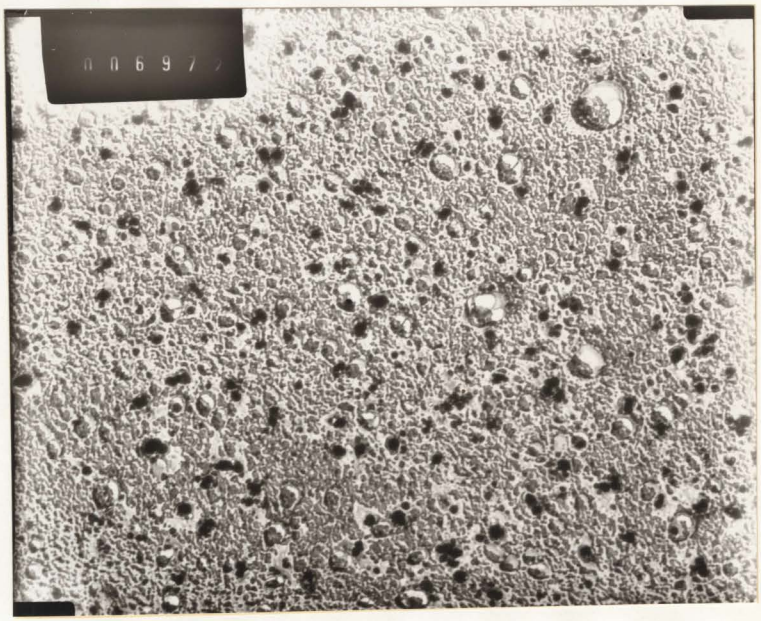

Figure 45

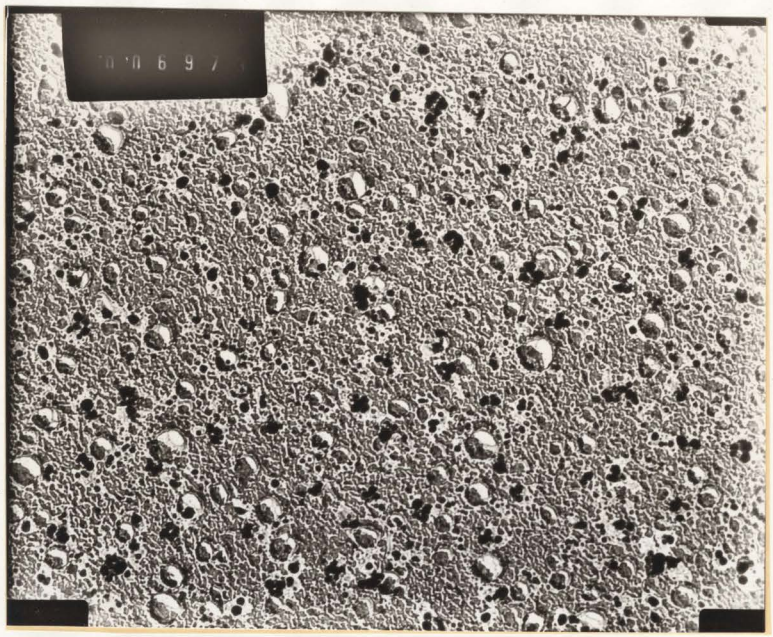

Figure 46

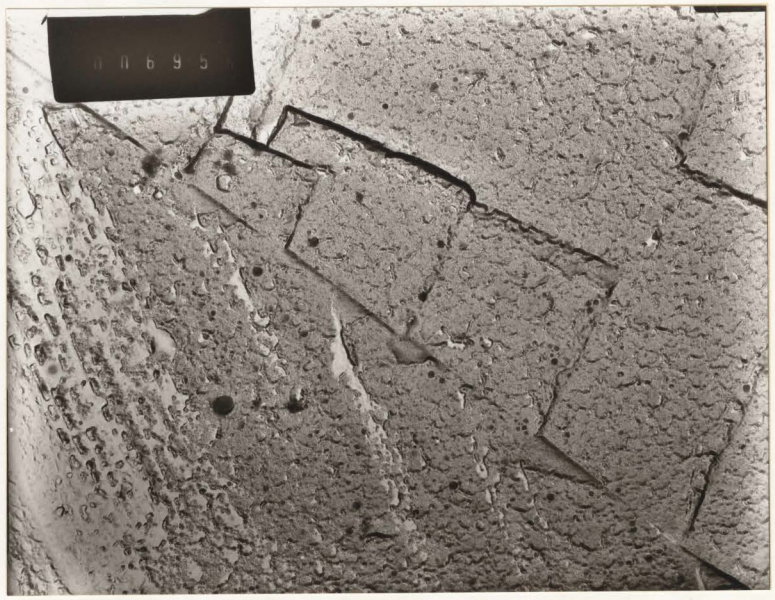

Figure 47

Figure 48

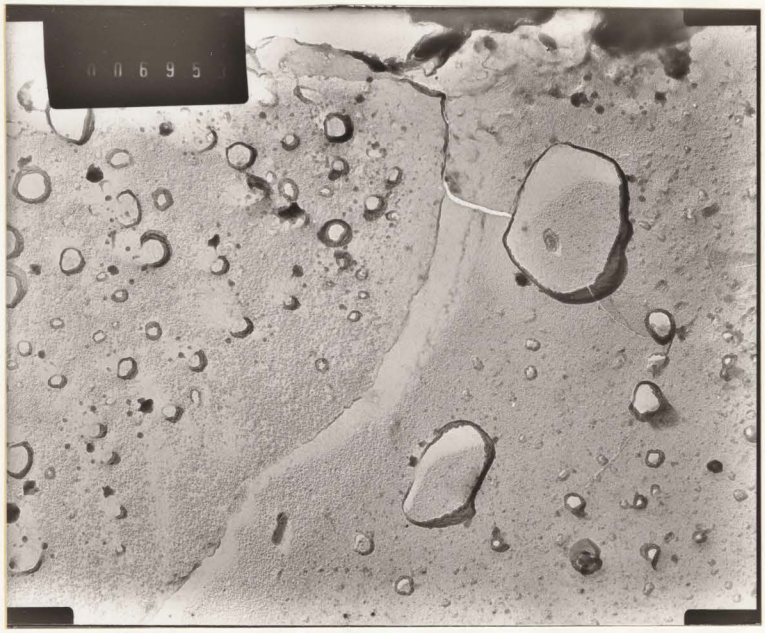

Figure 49

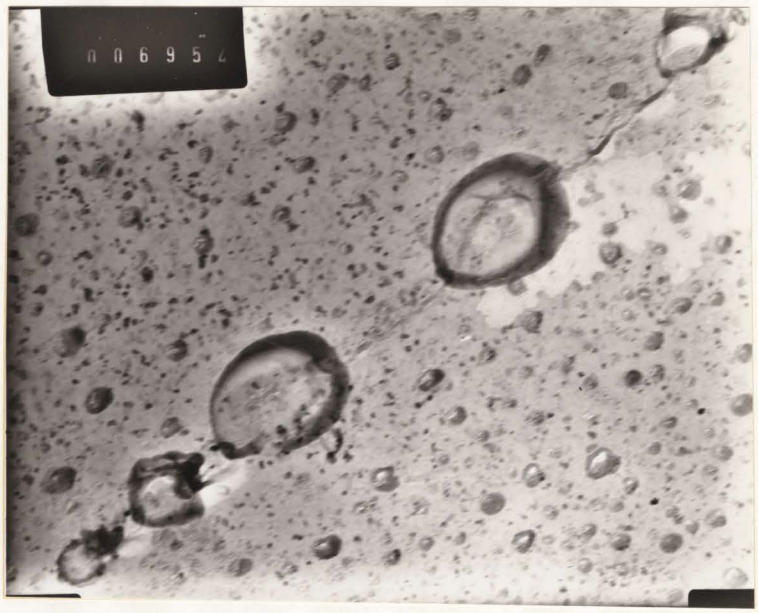

Figure 50

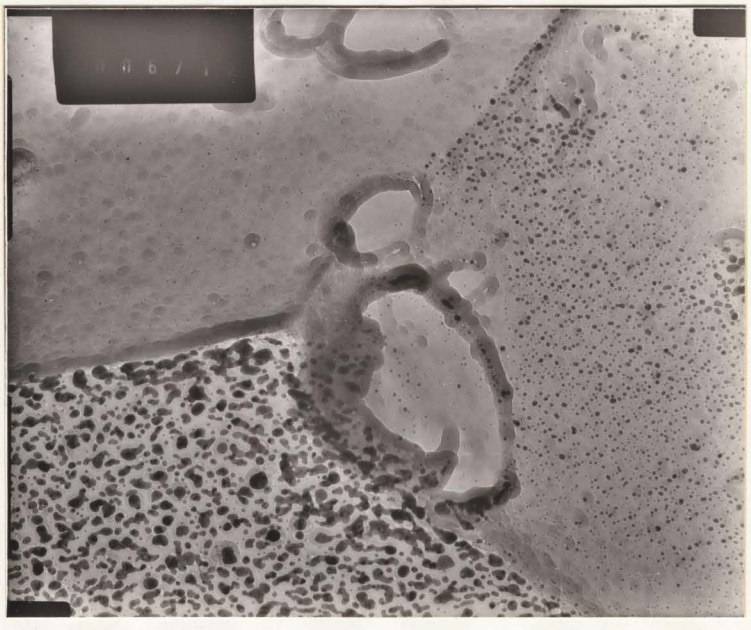

Figure 51

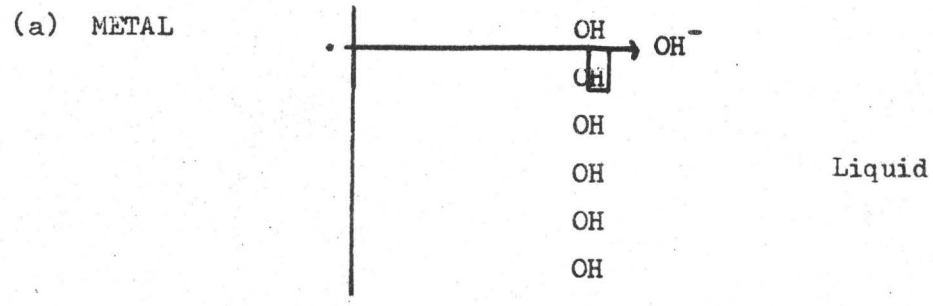

Figure 52a Early Stages

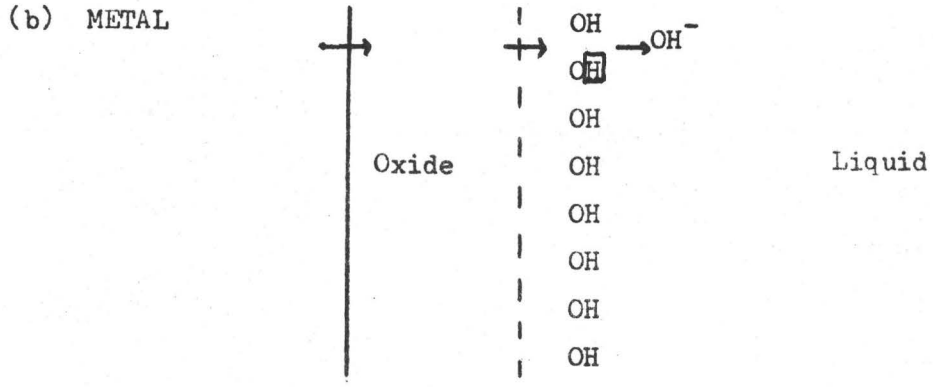

Figure 52b Later Stages

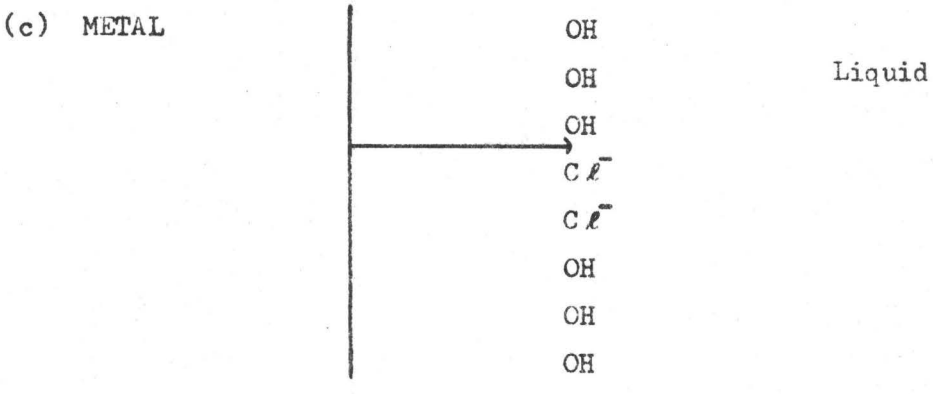

Figure 52c Action of Chlorine

Figure 52 Schematic Representation of Corrosion in Alkaline Media due to Contamination with Chlorine Ions.